

From the Klinik für Angeborene Herzfehler und Kinderkardiologie  
(Director: Prof. Dr. med. Anselm Sebastian Uebing)  
at the University Medical Center Schleswig-Holstein, Campus Kiel  
at Christian-Albrechts-Universität zu Kiel – Kiel University

**Serial right ventricular assessment in patients with hypoplastic left heart  
syndrome (HLHS): a multiparametric cardiovascular magnetic resonance study**

Dissertation  
to acquire the doctoral degree (Dr. med.)  
at the Faculty of Medicine  
at Christian-Albrechts-Universität zu Kiel – Kiel University

Written by  
**Mohamed Sobh**  
from Damietta, Egypt  
Kiel (2024)

1. Berichterstatter: **Prof Dr. med. Inga Voges**

2. Berichterstatter: **Prof. Dr. Tim Attmann**

Zum Druck genehmigt, Kiel, den

Tag der mündlichen Prüfung: **05.06.2025**

## Table of Contents

Table of Contents .....	I
Abbreviations .....	III
List of Figures.....	V
List of Tables.....	VI
<b>1. Introduction .....</b>	<b>Error! Bookmark not defined.</b>
1.1 Hypoplastic left heart syndrome (HLHS) .....	<b>Error! Bookmark not defined.</b>
1.1.1 Treatment of patients with HLHS.....	<u>3</u>
1.1.1.1 Initial treatment after birth .....	3
1.1.1.2 Surgical palliation .....	3
1.1.1.3 Heart transplantation .....	<u>7</u>
1.1.2 Outcome of patients with HLHS .....	7
1.1.2.1 Survival .....	7
1.1.2.2 Long-term follow-up .....	8
1.2 Single systemic right ventricular function and physiology.....	9
1.2.1 RV physiology and dysfunction in HLHS .....	9
1.2.2 Studies that have evaluated RV function in HLHS .....	<u>10</u>
1.3 Evaluation of systemic right ventricular function .....	<u>11</u>
1.4 The aim of the work.....	<u>15</u>
<b>2. Methods.....</b>	<b>16</b>
2.1 Study population.....	16
2.2 Ethical considerations .....	16
2.3 CMR acquisition .....	17
2.4 CMR analysis .....	17
2.5 Statistical analysis and reproducibility .....	18
<b>3. Results .....</b>	<b>20</b>
3.1 Patients .....	20
3.1.1 Patient basic data.....	20
3.1.2 Cardiac medication .....	22
3.2 Cardiovascular MRI.....	24
3.2.1 Right ventricular volumes and mass.....	24
3.2.2 Right ventricular ejection fraction and LAS .....	27

3.3 Reproducibility of right ventricular measurements .....	31
<b>4. Discussion</b> .....	<b>32</b>
4.1 Importance of ventricular function in HLHS and other single ventricle patients.....	32
4.2 Methods to evaluate ventricular function in single ventricle patients.....	32
4.3 Serial changes in RV volumes and mass .....	34
4.4 Serial changes in RV ejection fraction and LAS.....	35
4.5 Limitations.....	37
<b>5. Summary</b> .....	<b>39</b>
<b>6. List of Literature</b> .....	<b>41</b>
<b>7. CV</b>	

## Abbreviations

<b>AA</b>	Aortic atresia
<b>ACEI</b>	Angiotensin converting enzyme inhibitor
<b>AHA</b>	American heart association
<b>AR</b>	Aortic regurgitation
<b>AS</b>	Aortic stenosis
<b>ATP</b>	Adenosine triphosphate
<b>BMI</b>	Body mass index
<b>BSA</b>	Body surface area
<b>CHD</b>	Congenital heart disease
<b>CI</b>	Confidence interval
<b>CMR</b>	Cardiac magnetic resonance
<b>EF</b>	Ejection fraction
<b>HF</b>	Heart failure
<b>HLHS</b>	Hypoplastic left heart syndrome
<b>HIF</b>	hypoxia-inducible factor
<b>ICC</b>	Intra-class correlation coefficient
<b>IQR</b>	Interquartile range
<b>LAS</b>	Long axis strain
<b>LV</b>	Left ventricle
<b>MA</b>	Mitral atresia
<b>MS</b>	Mitral stenosis
<b>PA</b>	Pulmonary artery
<b>PGE1</b>	Prostaglandin E1
<b>RV</b>	Right ventricle
<b>RVEDV</b>	RV end-diastolic volume
<b>RVESV</b>	RV end-systolic volume
<b>RVEDVi</b>	RV end-diastolic volume index
<b>RVESVi</b>	RV end-systolic volume index
<b>RVMM</b>	Right ventricular myocardial mass
<b>RVMMi</b>	Right ventricular myocardial mass index
<b>SRV</b>	Systemic right ventricle

<b>TAPSE</b>	Tricuspid annular plane systolic excursion
<b>TCPC</b>	Total cavopulmonary connection
<b>TR</b>	Tricuspid regurgitation
<b>Y</b>	Year

## List of Figures

Figure 1.	Spectrum of hypoplastic left heart syndrome .....	2
Figure 2.	Stage 1 palliation of hypoplastic left heart syndrome .....	4
Figure 3.	Stage 2 procedure .....	5
Figure 4.	Completion of the Fontan circulation .....	6
Figure 5.	Right ventricular volumetry in a HLHS patient .....	13
Figure 6.	Assessment of long axis strain and tricuspid annular plane systolic excursion .....	13
Figure 7.	RV indexed end-diastolic volumes during longitudinal follow-up .....	26
Figure 8.	RV indexed end-systolic volumes during longitudinal follow-up .....	27
Figure 9.	Relationship between RV function parameters (long-axis strain and ejection fraction) as well as between RV function parameters and indexed RV volumes.....	30

## List of Tables

Table 1.	Characteristics of studied HLHS patients .....	20
Table 2.	Patient findings at each CMR examination .....	21
Table 3.	Frequency of tricuspid and aortic regurgitation at the time of CMR examination .....	22
Table 4.	Cardiac medications used at the time of each CMR examination .....	23
Table 5.	Serial changes of RV volumes and mass at the time of CMR examination .....	24
Table 6.	Comparison of RVEDVi at the three examinations expressed as P values of the Wilcoxon rank-sum tests for patients less and older than 10 years and for males & females .....	25
Table 7.	Comparison of RVESVi at the three examinations for patients less and older than 10 years and for males and females .....	26
Table 8.	CMR functional parameters at the time of each examination .....	28
Table 9.	Relationship between right ventricular volumes and functional parameters .....	29
Table 10.	Interobserver variability .....	31

# 1. Introduction

## 1.1 Hypoplastic left heart syndrome (HLHS)

Hypoplastic left heart syndrome (HLHS) is one of the most severe forms of congenital heart disease (CHD). The term describes a spectrum of left heart under development (Figure 1) (Graupner et al., 2019). HLHS is the most common form of functional single ventricle heart disease, with a birth prevalence of approximately 2 to 3 cases per 10,000 live births in the United States (Reller et al., 2008) and constitutes 1% to 2% of all cardiac malformations (Leirgul et al., 2014).

It is characterised by hypoplasia of the left ventricle (LV) and multilevel obstruction of systemic cardiac output from the level of the mitral valve to the proximal descending thoracic aorta. The anatomic variants of the disease can be distinguished by the status of the mitral and aortic valves resulting in a classification system that is described below.

The mitral atresia and aortic atresia (MA-AA) subtype is the most extreme of HLHS, accounting for 36% to 46%. There is either an absent or a slit-like LV cavity and diminutive ascending aorta (Rathod et al., 2022) (Tweddell JS et al., 2021).

The second subtype is characterised by mitral stenosis and aortic atresia (MS-AA) and occurs in conjunction with a severely hypoplastic ascending aorta. Depending on the degree of mitral stenosis, LV pressures may be subsystemic, systemic, or even suprasystemic. The degree of ventricular hypertrophy is also variable, but there is usually severe LV systolic dysfunction.

The third subtype comprises mitral stenosis and aortic stenosis (MS-AS). At the mildest end of the spectrum is the "borderline left heart", in which both valves are stenotic but not atretic. In some patients with MS-AS, the mitral and aortic valves are near-normal in size but a combination of LV diastolic and systolic dysfunction, or valvar stenosis, results in inadequate

LV systemic output. (Figure 1). After birth the systemic circulation is driven by the right ventricle (RV) via a patent ductus arteriosus. Without intervention, HLHS is fatal (**Rathod et al., 2022**).

At present, many infants with HLHS receive a prenatal diagnosis, which allows planning of delivery and treatment. The impact of prenatal diagnosis on surgical outcomes, however, remains controversial (**Bautista-Hernandez et al., 2019**).

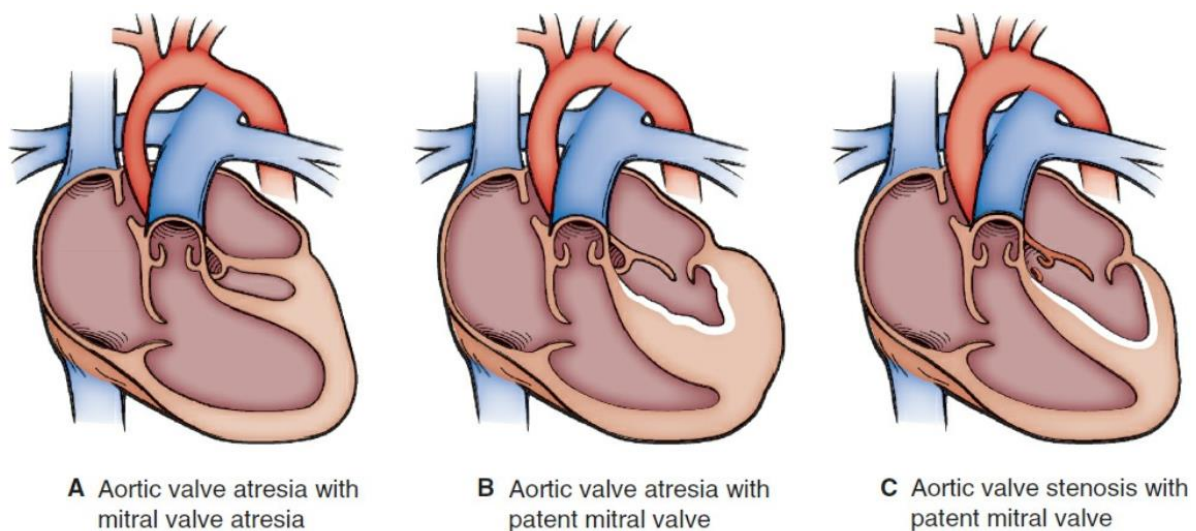


**Figure 1:** Spectrum of hypoplastic left heart syndrome (**Tweddell JS et al., 2021**).

(A) Mitral atresia and aortic atresia. This is the most extreme form of HLHS.

(B) Mitral stenosis and aortic atresia.

(C) Mitral stenosis and aortic stenosis. There is considerable variability in the size of the LV.

Echocardiographic imaging, whether pre- or postnatal, is sufficient in most cases to make a diagnosis of HLHS (**Alabdulgader., 2018**). During all stages of palliation, children with HLHS are at risk of circulatory failure and mortality. UK survival estimates corresponding to cases born between 2000 and 2015 were improved at 56%, but survival was examined up to age five only (**Best et al., 2021**).

## **1.1.1 Treatment of patients with HLHS**

### **1.1.1.1 Initial treatment after birth**

Neonates with HLHS are critically ill and will need to be managed in the intensive care unit and stabilised before surgical intervention during the first week of life. Initial management will include **(Kritzmire and Cossu, 2022)**: (1) maintaining ductal patency, (2) avoid excess pulmonary blood flow, and (3) ensure adequate blood flow from the left atrium to the right atrium **(Rao, 2019)**.

The immediate therapy for all infants with HLHS after birth is an intravenous infusion of low dose PGE1 to ensure ductal patency and maintain systemic circulation **(Akkinapally S et al., 2018)**. If a restrictive atrial septum is present, then the Rashkind procedure along with stent implantation might be a potential treatment option **(Rai et al., 2019)**.

### **1.1.1.2 Surgical palliation**

A three-stage surgical palliation is typically the treatment strategy of choice. The first stage takes place in the neonatal period and includes the Norwood operation or hybrid procedure, the second stage is the hemi-Fontan or Glenn operation performed at around 4–6 months of life, and the final stage is the completion of the Fontan circulation which is normally performed between 2-4 years of age **(Kolcz and Skalski, 2011)**.

#### **Norwood operation and hybrid procedure**

In many cardiac centers the Norwood operation in the neonatal period is the first operative stage. The aim of the Norwood operation is to use the RV as the main pumping ventricle for the systemic circulation. During the Norwood operation a so-called neo-aorta arising from the RV is created by using the patient's pulmonary valve and trunk and patch material (Figure 2A). The pulmonary blood flow is maintained by a modified Blalock-Taussig (Figure 2A)

shunt or a RV-to-pulmonary artery shunt (Sano modification, Figure 2B). The shunt is a long-term replacement for prostaglandin E1 (PGE1) administration and atrial septectomy is done to secure good atrial communication, which is required to permit pulmonary venous return to reach the RV (**Rai et al., 2019**).

The hybrid palliation expands the surgical options for patients born with HLHS. It consists of bilateral surgical pulmonary artery banding and percutaneous stenting of the Ductus arteriosus with or without atrial septum manipulation (**Schranz et al., 2015**; Figure 2B). The hybrid approach lessens the initial operative risk and is hypothesized to improve in particular neurological survival (**Licht et al., 2009**).

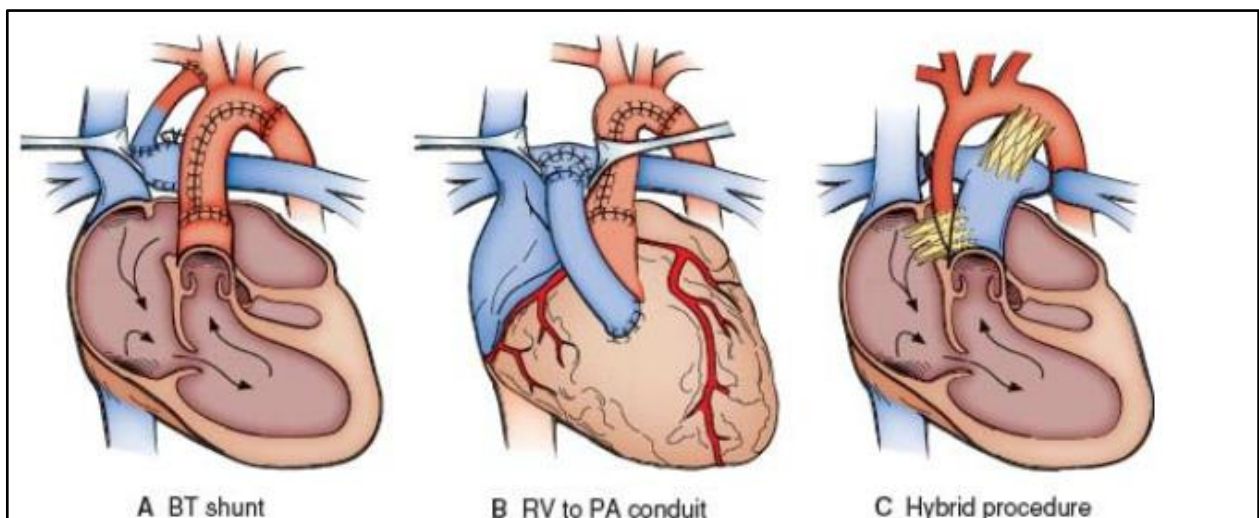


**Figure 2:** Stage 1 palliation of hypoplastic left heart syndrome (**Tweddell JS et al., 2021**).

A: Stage 1 palliation (Norwood procedure) using a modified Blalock–Thomas–Taussig (BT) shunt for provision of pulmonary blood flow.

B: Stage 1 palliation using RV-to-pulmonary artery conduit (Sano modification).

C: Stage 1 palliation using a hybrid approach. Pulmonary blood flow is restricted with branch pulmonary artery bands, and the ductal patency is maintained by placement of a stent. A stent is placed to create a nonrestrictive atrial septal defect.

### **Hemifontan operation and Glenn anastomosis**

The superior cavopulmonary connection is typically the second surgical step and involves the creation of an anastomosis between the superior vena cava and the pulmonary artery (Eckhauser et al., 2018). Currently, the bidirectional Glenn shunt and the hemi-Fontan procedure are the commonly used surgical options (Figure 3).

For the Glenn anastomosis the superior vena cava is divided and separated from the right atrium and an end-to-side anastomosis is made between the superior vena cava and the right pulmonary artery (Figure 3B). The hemi-Fontan operation includes creation of an anastomosis between the superior vena cava and the surgically augmented right pulmonary artery.

The entrance of the superior vena cava into the right atrium is closed with a patch (Edelson et al., 2020; Figure 3A).

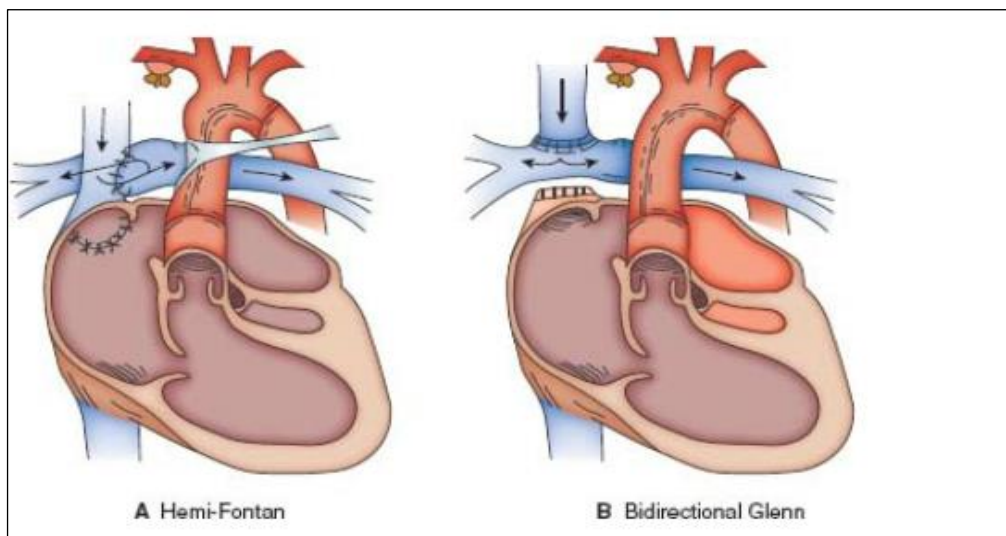


**Figure 3:** Stage 2 procedure (Tweddell JS et al., 2021).

**A:** The hemi Fontan procedure consists of an end-to-side anastomosis of the superior vena cava to the right pulmonary artery. The entrance of the superior vena cava into the right atrium is closed by a patch.

**B:** The bidirectional Glenn shunt is a direct anastomosis of the superior vena cava to the central pulmonary artery.

### Completion of the Fontan circulation

During the completion of the Fontan circulation the inferior vena cava is connected with the pulmonary artery using an intra-arterial lateral tunnel or extracardiac conduit with or without a fenestration between the tunnel or conduit and the atria (**Rai et al., 2019**; Figure 4).

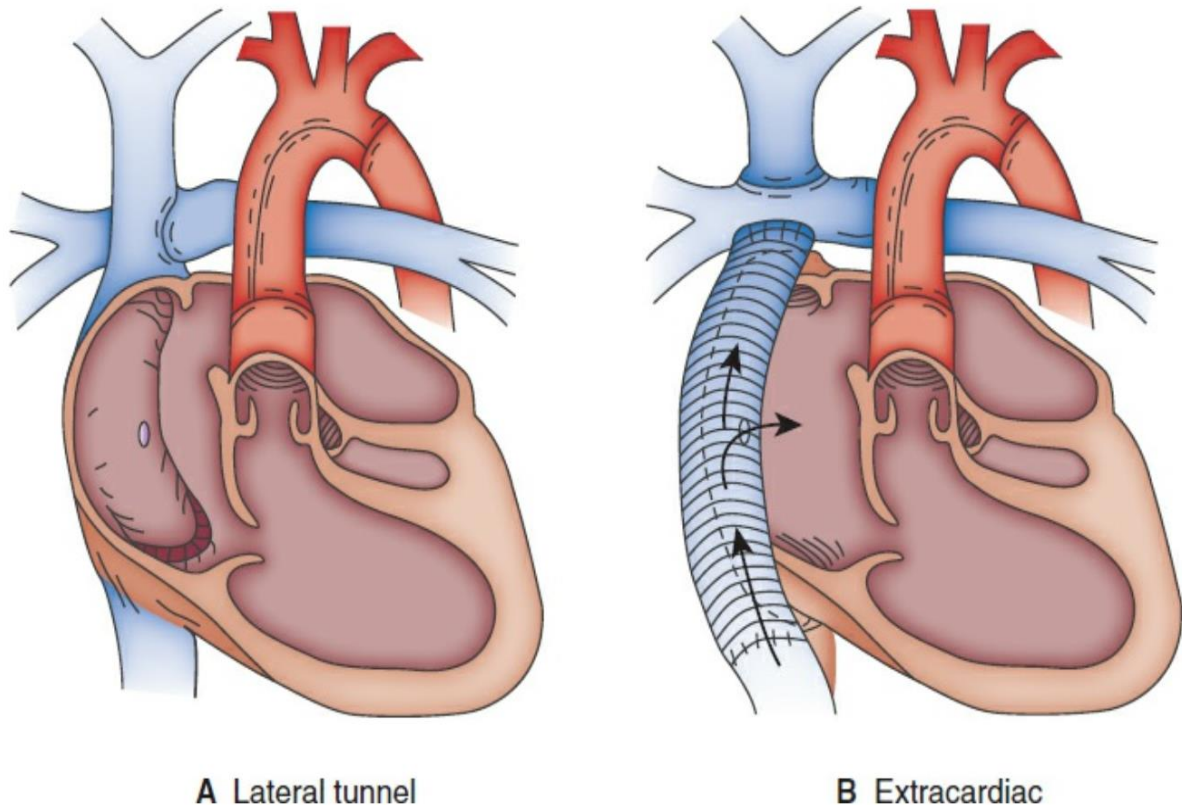


**Figure 4:** Completion of the Fontan circulation (**Tweddell JS et al., 2021**).

**A:** The lateral tunnel Fontan involves creating an intra-atrial baffle that connects the inferior vena cava to the pulmonary arteries.

**B:** The extracardiac Fontan uses a tube graft to connect the inferior vena cava to the central pulmonary artery. In both cases all caval return with the exception of the coronary sinus is directed to the pulmonary arteries, simulating as closely as possible the normal circulatory pattern. To improve hemodynamics, especially in the early postoperative period, a fenestration is often placed between the baffle or conduit and the pulmonary venous atrium. This decreases central venous pressure and increases preload to the single ventricle, albeit at the cost of some systemic desaturation.

### **1.1.1.3 Heart transplantation**

Although heart transplantation is a potential primary treatment option for newborns with HLHS, it is limited by the scarcity of donors. It is, however, a more commonly used treatment modality in cases of extreme heart failure during or after the three-stage surgical palliation, especially when the background is dysfunction of the right ventricle **(Rai et al., 2019)**.

## **1.1.2 Outcome of patients with HLHS**

### **1.1.2.1 Survival**

Only two-thirds of children with HLHS survive to 5 years of age **(Roeleveld et al., 2018)**. Recent studies show an overall survival of children with HLHS of 52% **(Siffel et al., 2015)**. Preterm infants had significantly poorer survival (31%) compared with term infants (56%) **(Erikssen et al., 2018)**.

Postoperative and long-term survival after Fontan procedure improved. By 15 to 20 years after Fontan procedure survival rates range from 60 to 85 percent and currently Fontan patients are predicted to have a 30-year survival rate of approximately 85 percent **(Johnson J,2022) (Ono M et al., 2006)**.

Fifteen years institutional experience with the Norwood procedure for patients with and without HLHS found that early and long-term survivals and postoperative complications were similar between patients with and without HLHS undergoing a Norwood operation. Recurrent aortic arch obstruction was common in both groups but more prevalent in patients without HLHS **(Hansen et al., 2012)**.

The Society of Thoracic Surgeons Congenital Heart Surgery Database (STS CHSD) reported in 2019 procedure mortality rates of stage I palliation 15%, Hemi-Fontan/Glenn 1.8%, and Fontan 1.0% **(Jacobs et al., 2019)**.

### **1.1.2.2 Long-term follow-up**

Long-term prognosis post Fontan completion has significantly benefit from the experience and technical developments of the past decades. However, postoperative long-term mortality and morbidity related to arrhythmias, thromboembolic events and protein-losing enteropathy as well as reoperations and reinterventions is concerning (**Kverneland LS, 2018**) (**Feinstein JA et al., 2012**). Regular cardiac follow-up and surveillance for early detection of potential complications and abnormalities will aid in decreasing the rates of failing Fontan (**Driscoll DJ et al., 1992**) (**Rychik J et al., 2019**).

Echocardiography should be part of every examination and is useful for the assessment of ventricular function, tricuspid regurgitation, thrombus formation and function of the neo-aortic root and valve as. Transesophageal echocardiography can visualise the entire Fontan pathway and might be helpful in thrombus detection (**Johnson J, 2022**).

Cardiovascular magnetic resonance imaging (CMR) plays an important role for the assessment of ventricular ejection fraction, cardiac output, visualisation of the Fontan pathways, branch pulmonary arteries as well as aorta and estimation of the impact of aortopulmonary collaterals on the Fontan circulation. Recently published American heart association (AHA) guidelines suggest that CMR should be performed every two to three years in Fontan patients (**Johnson J,2022**) (**Anderson RH et al., 2021**).

Cardiac catheterisation is indicated to investigate failing Fontan physiology and interventions. AHA guidelines suggest performing a cardiac catheterization at minimum every 10 years after the Fontan operation (**Johnson J, 2022**) (**Anderson RH et al., 2021**) (**Ono M et al., 2006**).

Annual electrocardiogram (ECG) is recommended to evaluate heart rhythm, further arrhythmia assessment may include Holter monitoring, event monitoring, prolonged rhythm

assessment, or exercise ECG to assess heart rate response and heart rhythm with exercise **(Johnson J, 2022) (Stout KK et al., 2019)**.

Annual chest radiography and cardiopulmonary exercise testing are generally suggested every one to three years **(Johnson J, 2022) (McCrindle BW et al., 2007)**.

Additional diagnostic tests such as markers of neurohumoral activation (N-terminal pro B-type natriuretic peptide, NT-pro BNP) and lung function tests are recommended for follow-up **(Budts et al., 2016) (Samarai et al., 2020) (Schneider et al., 2020)**.

## **1.2. Single systemic right ventricular function and physiology**

### **1.2.1. Right ventricular physiology and dysfunction in HLHS**

From even before birth, the single systemic right ventricle (SRV) is subject to abnormal hemodynamic demands and morphological abnormalities that can predispose to systolic or diastolic dysfunction. Palliation of the single ventricle with an aortopulmonary shunt or pulmonary artery band in the neonatal period results in increased ventricular volume load, a condition caused by the presence of pulmonary and systemic circulations existing in parallel, with mixing within the single ventricle. Valvular regurgitation (atrioventricular or semilunar) can also add to the hemodynamic stress on the myocardium. As a result of intracardiac mixing, arterial oxygen saturation is low, and the myocardium is subject to a chronically hypoxic environment **(Rychik et al., 2019) (Anderson et al., 2008)**.

Another reason for RV dysfunction might be disturbed myocardial fiber arrangement as well as the presence and extent of myocardial fibrosis associated with dilated and hypertrophied systemic ventricles, systolic dysfunction, regional wall motion abnormalities, and non-sustained ventricular tachycardia **(Rathod et al., 2010)**.

At the time when the Fontan procedure is performed, the ventricle commonly evolves from being volume overloaded, overgrown, and overstretched to volume deprived with a smaller cavity and increased wall thickness (**Rychik et al., 2019**).

There are two types of HF in Fontan patients. They present as the classic ventricular pump failure and the Fontan circulatory failure. The latter relates to the chronic increased central venous pressure and low cardiac output but with a remaining acceptable ventricular function. The systolic and diastolic ventricular function are relatively preserved during the first decades after Fontan completion but decline over time (**Atz et al., 2017**). Systolic dysfunction is present in 40–60% of patients considered for heart transplantation (**Miller et al., 2016**).

Because of remarkable surgical and medical advances over the past several decades, there are growing numbers of infants and children living with single ventricle CHD. Nevertheless, cardiac dysfunction (and ultimately HF) is a common complication in the single ventricle population, and pharmacological HF therapies have largely been ineffective in mitigating the need for heart transplantation (**Garcia et al., 2020**).

### **1.2.2. Studies that have evaluated RV function in HLHS**

A study from Bellsham-Revell et al. investigated changes in ventricular volumes and vascular dimensions before hemi-Fontan and before Total cavopulmonary connection (TCPC) in children with HLHS using CMR (**Bellsham-Revell HR et al., 2013**). The authors found that in HLHS, serial CMR imaging is well-suited to show the adaptation of the SRV after hemi-Fontan operation with volume reduction in the context of a preserved stroke volume and an increased ejection fraction.

Michel et al. assessed changes in systolic and diastolic RV function within a 5-year follow-up period of HLHS patients after TCPC using conventional and two-dimensional speckle tracking echocardiography showed the Systolic and diastolic RV function parameters of HLHS patients

decreased from 1.6 to 5.1 years after TCPC (**Michel MM et al., 2016**). Changes in global strain rate parameters may be signaling early RV dysfunction that is not detectable by traditional echocardiography.

In a cohort of clinically stable Fontan patients to assess longitudinal Fontan hemodynamics using serial CMR data and to study the impact of aortopulmonary collateral flow and type of single ventricle morphology revealed no significant changes in single ventricle dimensions and myocardial performance while aortopulmonary collateral flow decreased spontaneously (**Latus H et al., 2020**).

### **1.3 Evaluation of systemic right ventricular function**

Accurate evaluation of RV volumes and function in HLHS patients forms an essential aspect of surgical planning, peri-operative care and long-term management. The RV is volume loaded in the period after Norwood operation and before creation of a superior cavo-pulmonary connection, and there is often tricuspid regurgitation. Additionally, the size and shape of the accompanying hypoplastic left ventricle is variable and has a significant impact on RV geometry. Furthermore, the RV is in an anterior position and that may limit acoustic windows (**Bell et al., 2014**) (**Salehi et al., 2018**) (**Zaidi et al., 2018**).

Reliable quantification of the ventricular function is difficult in patients with a single ventricle physiology because of the complex diverse anatomy and lack of normal reference values and functional indexes for a non-left systemic ventricle (**Meyer et al., 2020**). There is no clear EF cut-off value that defines abnormal EF in SRV. This has also an impact on treatment strategies as it might be difficult to define the appropriate timing for initiating heart failure treatment, especially in asymptomatic CHD patients. In most cases, RV dysfunction by non-invasive imaging precedes the onset of clinical HF (**Santens et al., 2020**).

In clinical practice, echocardiography is predominantly used for the assessment of RV function, as it is non-invasive, widely available, relatively inexpensive, and has no adverse side effects. However, because of complex geometry, the assessment of SRV function by echocardiography has remained mostly qualitative (**Iriart et al., 2016**). Two-dimensional speckle tracking echocardiography parameter global longitudinal strain rate has been suggested as possible preload independent parameter of systemic RV contractility in HLHS after TCPC (**Husain et al., 2013**) (**Schlangen et al., 2014**). Zaidi et al. reported that echocardiographic measures could distinguish between HLHS patients with and without reduced RV function (**Zaidi et al., 2018**).

#### **CMR assessment of RV function**

The reference method for the assessment of RV volumetric function is CMR imaging. It provides high-resolution 3D images of the RV, which enable accurate assessments of RV systolic and diastolic volumes, which can then be used to calculate EF (**Abouzeid et al., 2017**). In addition, it allows a detailed assessment of the cardiovascular anatomy and myocardial structure and can evaluate blood flow parameters (**D'Alto et al., 2016**). However, CMR is time consuming, expensive, not universally available, cannot be used in some patients with claustrophobia and in some patients with cardiac pacemakers. CMR is the gold standard for the measurement of ventricular volumes and EF, and it also allows to easily measure TAPSE and long axis strain (**Riffel et al., 2015**; Figure 5).

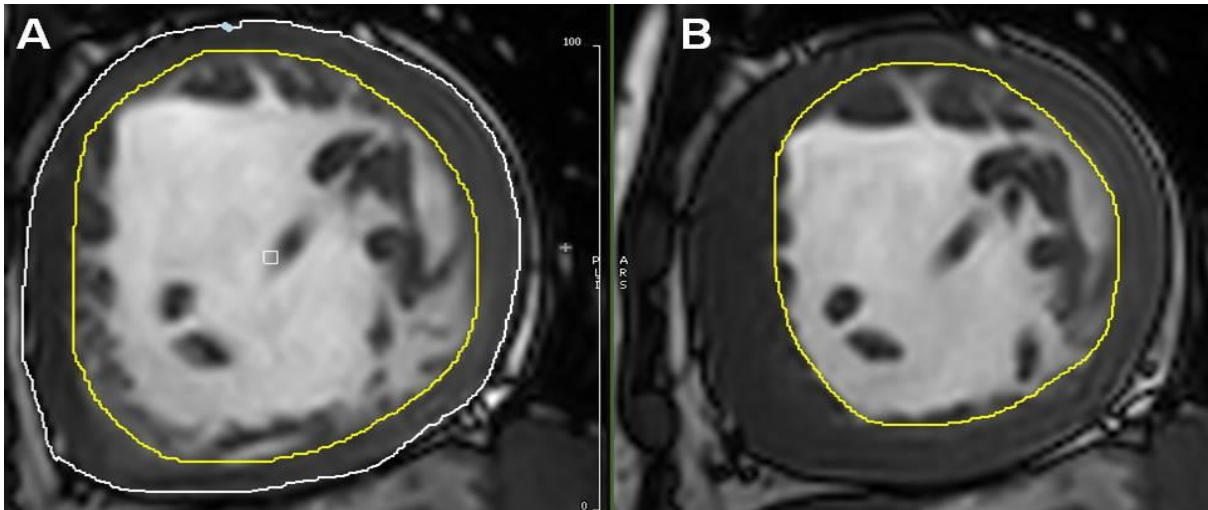


**Figure 5:** Right ventricular volumetry in a HLHS patient from short axis images at (A) end-diastole and (B) end-systole. (Sobh M et al., 2021).

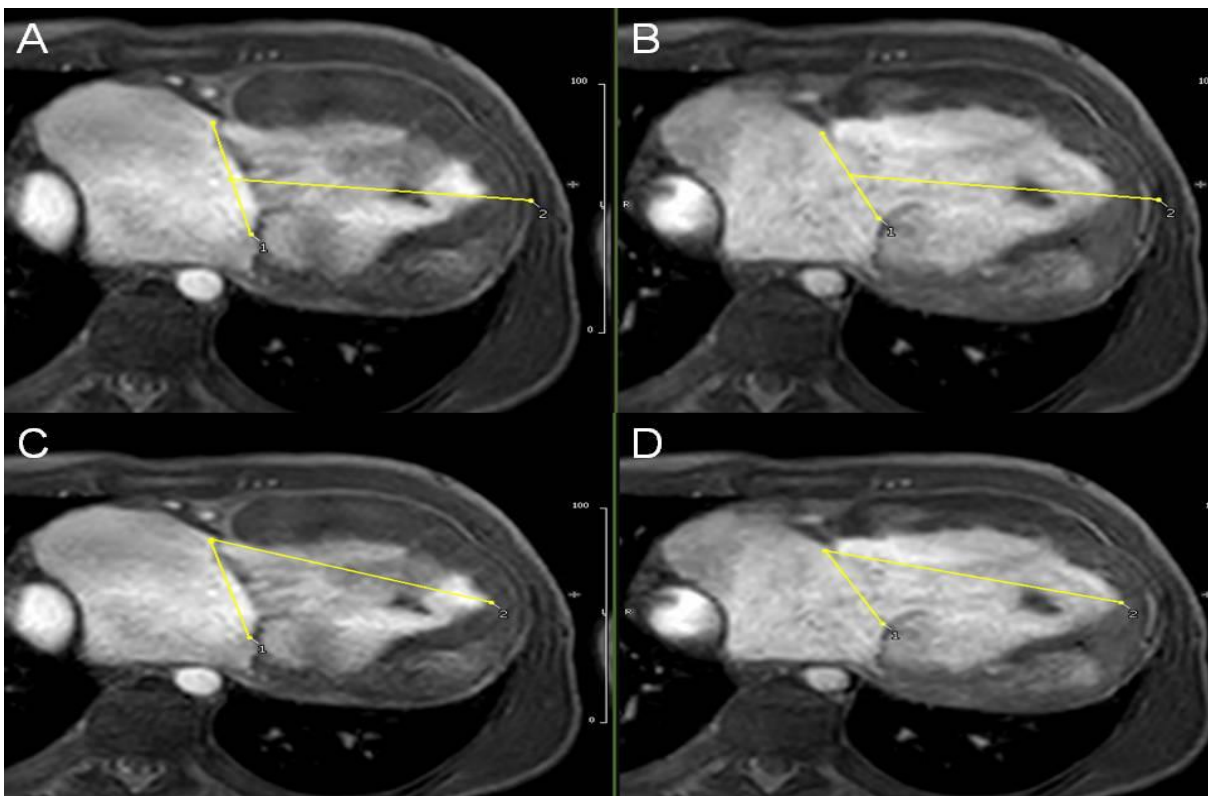


**Figure 6:** Long axis strain was assessed in a “4chamber-like view” by measuring the distance between the epicardial border of the LV apex and the middle of a line connecting the origins of the tricuspid valve leaflets in both (A) end-systole and (B) end-diastole. C+D) Tricuspid annular plane systolic excursion was assessed by measuring the largest distance between the

lateral tricuspid annulus and the right ventricular apex at (C) end-systole and (D) end-diastole **(Sobh M et al., 2021)**.

TAPSE is obtained from a standard apical four-chamber view and measures systolic excursion of the RV annular segment along its longitudinal plane. The greater the RV systolic excursion measurement, the greater the function of the RV. Measurement of the RV systolic function by using TAPSE is simple, less dependent on optimal image quality, and fairly reproducible. However, the measurement is made in a SRV segment to represent a complex 3D structure. Limitations include angle dependence, technical issues such as alignment difficulties, and a lack of validation in non-sinus rhythm **(Abouzeid et al., 2017; Figure 6)**.

Long axis strain in CMR analysis as a reliable and fast assessable parameter for RV global longitudinal function and has been shown to be valuable screening tool for patients with concomitant RV dysfunction in the clinical routine **(Arenja et al., 2016; Figure 6)**.

#### **1.4 The aim of the work**

HLHS is a complex form of congenital heart disease defined by anatomic and functional inadequacy of the left side of the heart. Following birth, surgical palliation is undertaken through staged operations comprising of the Norwood operation (or hybrid procedure) in the first week of life, creation of a superior cavopulmonary connection at 4-6 months of life, and finally completion of a TCPC at 2-4 years of age. Children with HLHS are at risk of various complications including dysfunction of the SRV.

In patients with HLHS RV dysfunction is common. However, only few studies exist that have evaluated RV function during serial follow-up after Fontan completion. The present work aimed to fill this gap by assessing RV volumes and RV functional markers from serial CMR studies in a large cohort of HLHS patients after completion of the TCPC.

## **2. Methods**

### **2.1 Study population**

This retrospective single-center study was performed at the Department of Congenital Heart Disease and Paediatric Cardiology at the University Hospital Schleswig-Holstein, Campus Kiel. Paediatric and adult patients with HLHS who underwent routine clinical CMR imaging between December 2005 and June 2020 were included in the study.

Inclusion criteria were All HLHS patients who had at least 2 serial CMR studies after Fontan completion in that period with a four-chamber cine view to measure long-axis strain (LAS) and/or a complete stack of short-axis cines for RV volumetry were included. Exclusion criteria were (i) patients with only one CMR study and (ii) insufficient data sets for the analysis of RV volumes and/or LAS.

Ninety-five patients had two examinations and thirty-six patients had three CMR examinations. The median interval between the first and the second examination was 5.0 years (range 0.9-8.4 years) and between the second and third examination was 4.9 years (range 0.7-7.5 years). The oldest patient at the time of the third examination was 21 years. All patients underwent Fontan completion with TCPC at a mean age of  $2.7 \pm 0.8$  (0.9-5.4) years.

For 162 examinations in children, sedation with midazolam and propofol was performed. In sedated patients, heart rate, respiratory motion, oxygen saturation, and noninvasive blood pressure were monitored.

### **2.2 Ethical considerations**

The study protocol conforms to the ethical guidelines of the 1975 Declaration of Helsinki and was approved by the local ethics committee (Ref.-Nr.: D503/20). Informed consent was obtained from the parents or guardians of the children enrolled into the study.

## 2.3 CMR acquisition

CMR was performed using a 3T scanner (Philips Achieva and Philips Ingenia; Philips Health Systems, The Netherlands). Short-axis cine stacks were acquired using gradient echo or steady state free precession (SSFP) cine imaging with retrospective ECG gating, to measure RV volumes, myocardial mass and function. The scan parameters were as follows: field of view 180-400 mm, slice thickness 5-8 mm, 25 cardiac phases, no slice gap, non-breath-hold in sedated children, breath-hold in conscious patients. In addition, an oblique cine image showing the atria and right ventricle in a similar manner as a standard 4-chamber view was obtained with the following scan parameters: field of view 180-320 mm, slice thickness 5-8 mm, 25 cardiac phases, non-breath-hold in sedated children, breath-hold in conscious patients.

## 2.4 CMR analysis

Post-processing was performed using commercially available software (cvi42 for Cardiovascular MRI, Circle Cardiovascular Imaging, Calgary, Canada).

Assessment of RV volumes, myocardial mass and ejection fraction (RVEF) was performed by manual tracing of endocardial contours for each slice from the stack of short-axis cine images at end-systole and end-diastole using Simpson's method (**Leiner T et al., 2020**).

The position of the tricuspid valve was confirmed by linking the short-axis stack to a long-axis view of the RV. Trabeculations and papillary muscles were included into the ventricular volume (Figure 5). RV volumes were measured RVEDV, RVESV, RVSV, RVEF and RV mass. The RVSV and RVEF were measured according to the following formulas:

$$(1) \quad RVSV = RVEDV - RVESV$$

$$(2) \quad RVEF = \frac{RVEDV - RVESV}{RVEDV} \times 100$$

All ventricular volume and mass were indexed to body surface area (BSA).

In 89 patients, tricuspid regurgitant fraction was calculated from RV stroke volume and neo-aortic forward flow from phase contrast acquisitions and expressed as a percentage of the ventricular stroke volume. The degree of tricuspid regurgitation was documented and classified as none, trivial (regurgitant fraction <10%), mild (regurgitant fraction <30%), moderate (regurgitant 30-40%) and severe (**Devos DG et al., 2010**).

Long axis strain (LAS) was assessed from 4-chamber views by measuring the displacement of the tricuspid valve annulus. For this the distance between the epicardial border of the LV apex and the middle of a line connecting the origins of the tricuspid valve leaflets were measured in both end-systole and end-diastole. LAS was then measured and expressed as a percentage according to the following formula (**Riffel et al., 2015**):

$$(3) \text{ LAS [\%]} = \frac{\text{RV length end-systole} - \text{RV length end-diastole}}{\text{RV length end-diastole}} \times 100$$

Tricuspid annular plane systolic excursion (TAPSE) was measured by subtracting the distance between the lateral tricuspid annulus and the right ventricular apex in end-diastole from the same distance in end-systole (Figure 6 C+D).

In four patients, ventricular volumetry was not possible and in one patient the measurement of TAPSE and LAS was not performed, all because of poor image quality.

## **2.5 Statistical analysis and reproducibility (Sobh M et al., 2021)**

Statistical analysis was carried out by using SPSS (version 25) and R (version 3.50). As most of the continuous data were skewed distributed, they are shown as median with the first and third quartiles (always given in square brackets). Categorical variables are expressed as total counts with percentages. To detect possible confounding variables as gender or age, the

measured cardiological parameter at the first and the second examinations were compared between male and female patients, and between age groups (dichotomized at the median of 10 years) using independent Wilcoxon tests in an explorative manner, and, therefore, not adjusted for multiple testing.

Taking the impact of age on RV parameters into account, subsequent analyses of the primary end points were done for both age groups (below 10 years and above 10 years) separately: The difference in the RV end-diastolic volume index (RVEDVi) and in the RV end-systolic volume index (RVESVi) from the first to the second examinations was analysed by a Wilcoxon signed-rank test, hypothesising that there are no changes over time. Similarly,

The difference between the first/second and the third examinations, where a total of 35 out of 95 patients were available, was analysed as well. Regarding the repeated measurements on the same patient over time, the significance level was adjusted by Bonferroni correction as follows (**VanderWeele TJ et al., 2019**) the global significance level of 5% was divided by the number of comparisons at 3 time points, which were additionally multiplied by 2 as considering the 2 volume indices (RVESVi, RVEDVi).

This calculation resulted in a corrected significance level of  $0.0083 = 0.05 / (3 \times 2)$ . Spearman's rank correlation was used to assess associations between RV size and functional parameters at the time of the second and third examinations. Intraclass correlation analysis was performed to measure interobserver variability (moderate  $<0.7$ , good  $\geq 0.7-0.9$  and excellent  $>0.9$ ).

### 3. Results

#### 3.1 Patients

##### 3.1.1 Patient basic data

Sixty patients had two CMR examinations and thirty-five patients had three CMR examinations. The median interval between the first and the second examination was 4.9 years (range 1.1-6.9 years) and between the second and third examination was 4.8 years (range 0.7-7.5 years). All patients underwent Fontan completion with TCPC at a median age of 2.7 [1st quartile 2.2; 3rd quartile 3.1] (range 1.5-5.2) years. Forty patients (42.1 %) had (MA-AA), thirty patients had (MS-AS) (31.6 %), twenty patients had (MS-AA) (21.1 %) and five patients had (MA-AS) (5.3 %) (Table 1).

**Table 1.** Characteristics of studied HLHS patients (n=95)

Variables	HLHS patients (n= 95)	
	NO.	%
Male	66	69.5
Female	29	30.5
<b>No. of patients with completed CMR scans:</b>		
Two scans	60	63.2
Three scans	35	36.8
<b>HLHS spectrum:</b>		
MA-AA	40	42.1
MS-AS	30	31.6
MS-AA	20	21.1
MA-AS	5	5.3
	<b>Median [IQR]</b>	
<b>Age at Fontan completion with TCPC (years)</b>	2.7 [2.2; 3.1]	
<b>Interval between scans (years)</b>		
1 <sup>st</sup> and 2 <sup>nd</sup> scan	4.9 [3.5-5.6]	
2 <sup>nd</sup> and 3 <sup>rd</sup> scan	4.8 [3.9-5.7]	

IQR, interquartile range; MA-AA, aortic atresia and mitral atresia; MA-AS, mitral atresia and aortic valve stenosis; MS-AA, mitral stenosis and aortic valve atresia; MS-AS, mitral and aortic valve stenosis.

Median age and interquartile range (IQR) of included patients at the three examinations was 4.2 [3.3; 6.1] years, 9.4 [5.7; 11.4] years and 14.6 [11.8; 16.8] years. The oldest patient at the time of the third examination was 21.2 years. Median weight at the time of first CMR examination was 16 kg while at the time of third examination was 50 kg. Changes in anthropometric measures through CMR examinations are summarized in Table 2.

**Table 2:** Patients findings at each CMR examination

<b>Variables</b>	<b>1<sup>st</sup> CMR after</b>	<b>2<sup>nd</sup> CMR after</b>	<b>3<sup>rd</sup> CMR after</b>
	<b>TCPC completion (n= 95)</b>	<b>TCPC completion (n= 95)</b>	<b>TCPC completion (n= 35)</b>
	<b>Median (IQR)</b>	<b>Median (IQR)</b>	<b>Median (IQR)</b>
<b>Age (y)</b>	4.2 [3.3;6.1]	9.4 [5.7;11.4]	14.5 [10.4;16.8]
<b>Weight (kg)</b>	16 [13.6;18.7]	27.5 [20;34]	50 [34;60.5]
<b>Weight centile</b>	50 (<5-95)	50 (<5-95)	50 (<5-95)
<b>Height (cm)</b>	101.0 [93;111]	130.9 [114;145]	160 [147;171.5]
<b>Height centile</b>	25 (<5-95)	50 (<5-95)	50 (<5-95)
<b>BMI (kg/m<sup>2</sup>)</b>	15.7 [14.5;16.8]	16.0 [14.7;17.8]	18.9 [16.5;23.3]
<b>BSA (m<sup>2</sup>)</b>	0.7 [0.6;0.7]	1.0 [0.8;1.2]	1.5 [1.2;1.7]

BMI; Body mass index; BSA, body surface area; IQR, interquartile range; y, year.

For patients with a height or weight below the 5<sup>th</sup> centile, we used the value 1 to calculate the median centile.

One patient had mild aortic stenosis at the proximal anastomosis of the neo-aorta at the time of the third examination. Nine patients had moderate TR at the time of first and third examinations while one patient had severe TR at the time of second examination as described

in Table 3. Moderate TR was associated with higher RVEDVi and RVESVi compared to less degrees of TR, but this difference was not significant. The degree of TR did not have any impact on RVEF and LAS.

**Table 3.** Frequency of TR, AR at the time of each examination

	1 <sup>st</sup> CMR after TCPC completion (n= 95)	2 <sup>nd</sup> CMR after TCPC completion (n= 95)	3 <sup>rd</sup> CMR after TCPC completion (n= 35)
<b>TR</b>			
- Trivial (n, %)	49 (51.7 %)	41 (43.2 %)	13 (37.1 %)
- Mild (n, %)	21 (23.6 %)	28 (29.5 %)	8 (22.9 %)
- Moderate (n, %)	9 (9.5 %)	11 (11.6 %)	9 (25.7 %)
- Severe (n, %)		1 (1.1 %)	
<b>AR</b>			
- Trivial (n, %)	45 (47.4)	52 (54.7)	19 (54.3)
- Mild (n, %)	32 (33.7)	22 (23.2)	10 (28.6)
- Moderate (n, %)	1 (1.1)	5 (5.3)	1 (2.8)
- Severe (n, %)		1 (1.1)	

**TR**, tricuspid regurgitation; **N**, number; **AR**, aortic regurgitation

### 3.1.2 Cardiac medication

Thirty-five patients (36.8%) were treated with angiotensin converting enzyme inhibitors (ACEI) at the time of the first examination. Indications were: 1) to lower systemic vascular resistance and to improve diastolic dysfunction after TCPC completion (n= 26 out of 35), 2) RV dysfunction, tricuspid regurgitation, or neo-aortic valve regurgitation (n= 9 out of 35). ACEI were continued in some patients due to RV dysfunction, arterial hypertension, tricuspid

regurgitation and neo-aortic valve regurgitation (second CMR examination: n= 17; third CMR examination: n= 11).

Betablockers were taken by eleven patients at the time of the first examination. At the time of the second examination seven patients and at the time of the third examination three patients were on betablockers in the context of RV dysfunction. Aspirin was taken by eighty-one patients at the time of the first examination and seventy-nine and twenty-five at the time of the second examination and the third examination respectively. A summary of the medication at the time of each examination is given in Table 4.

**Table 4.** Cardiac medications used at the time of each CMR examination

<b>Medications</b>	<b>1<sup>st</sup> CMR after</b>	<b>2<sup>nd</sup> CMR after</b>	<b>3<sup>rd</sup> CMR after</b>
	<b>TCPC completion</b> <b>(n= 95)</b>	<b>TCPC completion</b> <b>(n= 95)</b>	<b>TCPC completion</b> <b>(n= 35)</b>
	<b>NO. (%)</b>	<b>NO. (%)</b>	<b>NO. (%)</b>
<b>Aspirin</b>	81 (85.3)	79 (83.2)	25 (71.4)
<b>ACEI</b>	35 (36.8)	17 (17.9)	11 (31.4)
<b>Beta-blocker</b>	11 (11.6)	7 (7.4)	3 (8.6)
<b>Diuretics</b>	16 (16.8)	6 (6.3)	5 (14.3)
<b>Phenprocoumon</b>	13 (13.7)	13 (13.7)	4 (11.4)

ACEI: angiotensin converting enzyme inhibitor; TCPC, Total cavopulmonary connection; N, number

## 3.2 Cardiovascular MRI

### 3.2.1 Right ventricular volumes and mass

Serial changes of RV volumes and mass are described in table (5). Median RVEDV increased from 61.4 ml at the time of first examination to 89.8 ml at time of second examination to 156.6 ml at the time of third examination. Also, median RVESV increased through the three examinations from 27.9 ml to 39.4 ml to 71.6 ml. There was no significant change for indexed myocardial mass throughout the examinations.

**Table 5.** Serial changes of RV volumes and mass at the time of each CMR examination

Parameters	1 <sup>st</sup> CMR after TCPC completion (n= 95)	2 <sup>nd</sup> CMR after TCPC completion (n= 95)	3 <sup>rd</sup> CMR after TCPC completion (n= 35)
	Median [IQR]	Median [IQR]	Median [IQR]
<b>RVEDV (ml)</b>	61.4 [50.4; 72.8]	89.8 [69.2; 118.3]	156.6 [108.8; 198.7]
<b>RVESV (ml)</b>	27.9 [21.4; 34.3]	39.4 [29.7; 58.8]	71.6 [45.6; 96.0]
<b>RVEDVi (ml/m<sup>2</sup>)</b>	88.8 [76.3; 104.9]	<sup>a</sup> 89.7 [76.6; 105.7]	100.3 [85.8; 116.2]
<b>RVESVi (ml/m<sup>2</sup>)</b>	41.2 [30.7; 50.3]	<sup>a</sup> 41.0 [32.4; 50.5]	46.7 [39.6; 63.2]
<b>RVMM (g)</b>	58.9 [48.3; 74.0]	81.8 [59.5; 114.4]	134.1 [87.7; 182.4]
<b>RVMMi (g/m<sup>2</sup>)</b>	88.9 [67.9; 103.3]	84.8 [61.1; 106.9]	90.4 [66.7; 122.5]

EDV, end diastolic volume; ESV, end systolic volume; IQR, interquartile range; LAS, long axis strain; RV, right ventricle; RVEDVi, right ventricular end diastolic volume index; RVESVi, right ventricular end systolic volume index; RVMM, right ventricular myocardial mass; RVMMi, right ventricular myocardial mass index;

a significant difference between age groups in the change from the 1<sup>st</sup> CMR examination compared to the 2<sup>nd</sup> CMR, tested by Wilcoxon test for independent samples,  $p < 0.05$ .

There was a significant increase in RV indexed end-systolic and end-diastolic volumes (RVEDVi, RVESVi) from the first to the second as well as from the first and the second examination to the third examination in patients with an age >10 years. Gender did not impact the changes of RV volumes across the examinations as shown in Table 6 & 7 and illustrated in Figure 7 & 8.

**Table 6.** Comparison of RVEDVi at the three examinations expressed as P values of the Wilcoxon rank-sum tests for patients less and older than 10 years and for males and females

Age group	RVEDVi 1 - RVEDVi 2	RVEDVi 1 - RVEDVi 3	RVEDVi 2 - RVEDVi 3
Age<10	0.026 (n=39)	0.28 (n=10)	0.33 (n=10)
Age≥10	<0.001*(n=52)	<0.003* (n=25)	<0.004* (n=25)
Gender	RVEDVi 1 - RVEDVi 2	RVEDVi 1 - RVEDVi 3	RVEDVi 2 - RVEDVi 3
Male	0.7 (n=63)	0.11 (n=26)	0.01 (n=26)
Female	0.34 (n=28)	0.07 (n=9)	0.3 (n=9)

RVEDVi, right ventricular end diastolic volume index; \*significant after Bonferroni correction.

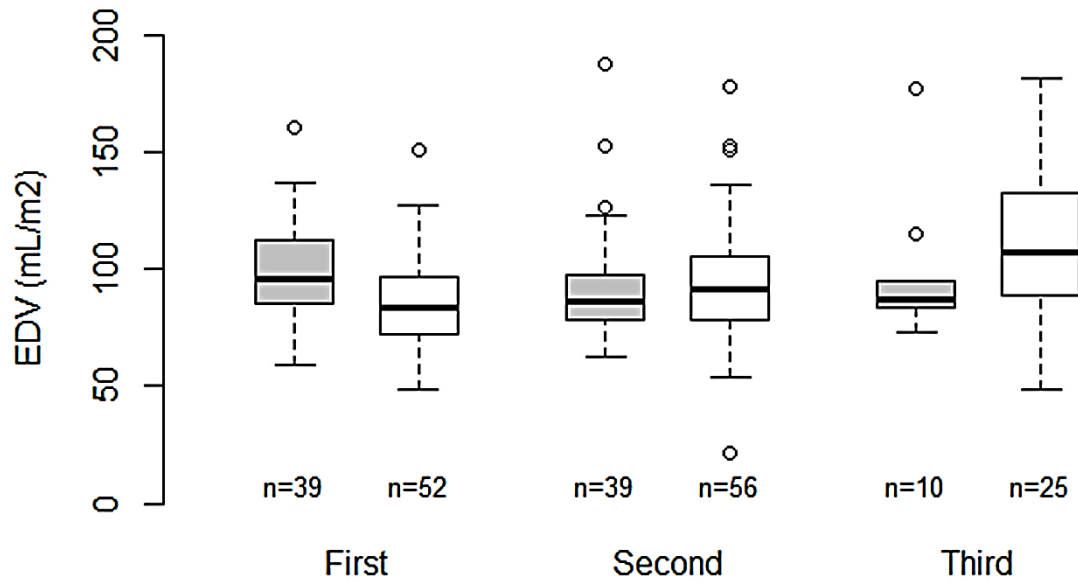


**Figure 7:** RV indexed end-diastolic volumes at the first, second and third examinations for children <10 years (grey box) and older or equal to 10 years (white box).  
EDV: end-diastolic volume.

**Table 7.** Comparison of RVESVi at the three examinations expressed as P values of the Wilcoxon rank-sum tests for patients less and older than 10 years and for males and females

Age group	RVESVi 1 - RVESVi 2	RVESVi 1 - RVESVi 3	RVESVi 2 - RVESVi 3
Age<10	0.115 (n=39)	0.24 (n=10)	0.88 (n=10)
Age≥10	<0.001* (n=52)	<0.001* (n=25)	<0.001* (n=25)
Gender	RVESVi 1 - RVESVi 2	RVESVi 1 - RVESVi 3	RVESVi 2 - RVESVi 3
Male	0.6 (n=63)	0.02 (n=30)	0.02 (n=30)
Female	0.09 (n=28)	0.068 (n=5)	0.13 (n=5)

RVESVi, right ventricular end systolic volume index; \*significant after Bonferroni correction.

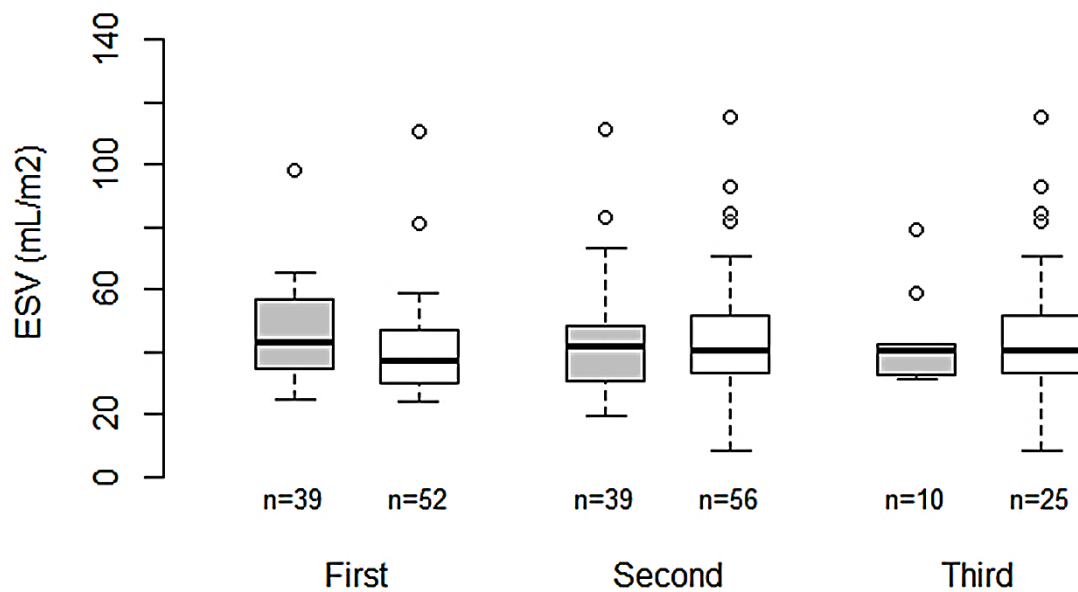


**Figure 8:** RV indexed end-systolic volumes at the first, second and third examinations for children <10 years (grey box) and older or equal to 10 years (white box).  
ESV: end-systolic volume.

### 3.2.2 Right ventricular ejection fraction and LAS

There was no significant change for indexed RV stroke volume throughout the examinations (48.4 [42;55.7], 47.6 [42.2;57.5], 49.7 [45.1;59.4]). Cardiac output and cardiac index were derived from RVSV. Serial changes of the RV ejection fraction, LAS (%) and TAPSE (mm) are described at Table 8. RVEDVi and RVESVi were correlated with RVEF and LAS (Table 9, Figure 9 B-E).

**Table 8.** CMR functional parameters at the time of each examination

<b>Parameters</b>	<b>1<sup>st</sup> CMR after TCPC completion (n= 95)</b>	<b>2<sup>nd</sup> CMR after TCPC completion (n= 95)</b>	<b>3<sup>rd</sup> CMR after TCPC completion (n= 35)</b>
<b>LAS (%)</b>	-9.3 [-7.0; -11.1]	-8.7 [-6.6; -11.0]	-8.9 [-5.5; -11.3]
<b>RVSV (ml)</b>	31.7 [29.3; 38.1]	48.2 [39.2;57.1]	73.3 [58.;89.0]
<b>RVEF (%)</b>	54.0 [50.0; 59.2]	54.0 [48.4;58.9]	52.6 [45.7;57.6]
<b>RVSVi (ml/m<sup>2</sup>)</b>	48.4 [42.0; 55.7]	47.6 [42.2;57.5]	49.7 [45.1;59.4]
<b>Cardiac index (l/min/m<sup>2</sup>)</b>	4.1 [3.2; 4.9]	3.7 [3.1;4.6]	4.0 [3.4;5.2]
<b>Heart rate (bpm)</b>	86.0 [78.0; 94.0]	81.0 [69.0;93.0]	79.0 [70.0;89.0]
<b>Cardiac output (l/min)</b>	2.8 [2.3; 3.2]	3.7 [3.1;4.5]	6.0 [4.5;7.4]
<b>TAPSE (mm)</b>	6.1 (4.9-7.9)	6.6 (5.1-9)	7.1 (4.9-8.9)

bpm, beats per minute; LAS, long axis strain; RVEF, right ventricular ejection fraction; RVSVi, right ventricular stroke volume index; SV, stroke volume; TAPSE, Tricuspid annular plane systolic excursion.

**Table 9.** Relationship between right ventricular volumes and functional parameters

<b>Parameters</b>	<b>RVEF (n=221)</b>		<b>RV LAS (n=220)</b>	
	<b>(Spearman's correlation)</b>		<b>(Spearman's correlation)</b>	
	<b>r</b>	<b>P-value</b>	<b>r</b>	<b>P-value</b>
<b>RVEDVi</b> <b>(ml/m<sup>2</sup>)</b>	-0.17	0.018	0.26	<0.001
<b>RVESVi</b> <b>(ml/m<sup>2</sup>)</b>	-0.32	<0.001	0.43	<0.001
<b>RVMMi</b> <b>(ml/m<sup>2</sup>)</b>	-0.08	0.3	0.20	0.002
<b>RVEF (%)</b>			-0.23	<0.01

LAS, long axis strain; N, number; RVEDVi, right ventricular end diastolic volume index; RVEF, right ventricle ejection fraction; RVESVi, right ventricular end systolic volume index; RVMMi, right ventricular myocardial mass index.

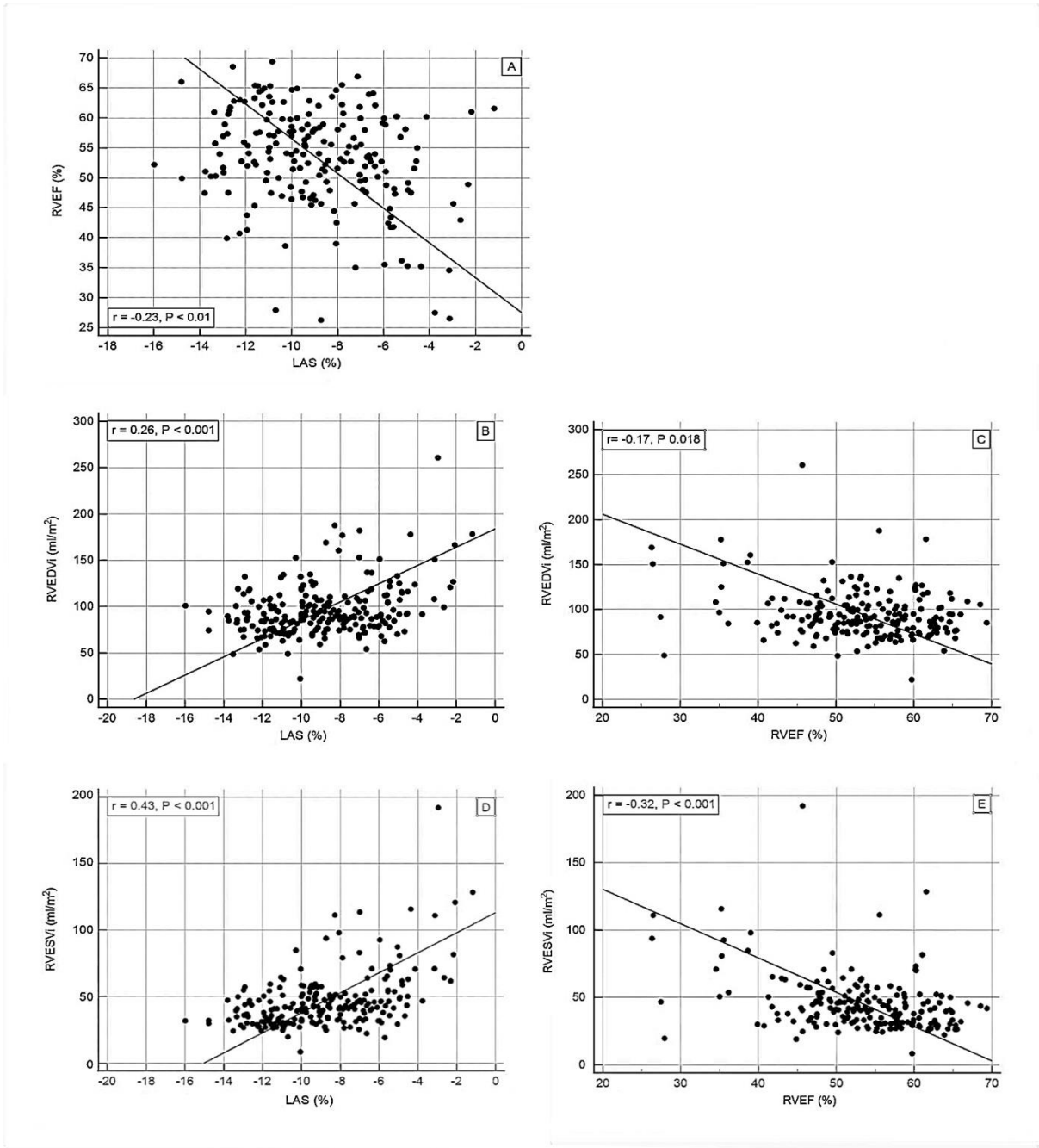


**Figure 9:** (A-B- D) Relationship between RV long-axis strain and indexed RV volumes as well as RV EF, ( C- E) Relationship between RV ejection fraction and indexed RV volumes . LAS: long-axis strain; RVEDVi: right ventricular end-diastolic volume index; RVEF: right ventricular ejection fraction; RVESVi: right ventricular end-systolic volume index.

### 3.3 Reproducibility of right ventricular measurements

Good-to excellent interobserver agreement was shown for all right ventricular measurements in 25 patients. The intra-class correlation coefficient ranged from 0.782 to 0.996 (Table 10).

**Table 10.** Intra-class correlation coefficients from interobserver assessment

	ICC	CI
RVEF	0.948	0.884-0.977
RVEDV	0.993	0.983-0.997
RVESV	0.996	0.990-0.998
RVSV	0.973	0.940-0.988
RVMM	0.964	0.918-0.984
LAS	0.782	0.510-0.903

ICC, intra-class correlation coefficient; CI, confidence interval

## 4. Discussion

Careful evaluation of the function of the systemic RV is important in children with HLHS after TCPC completion as early deterioration of RV function is expected. In this CMR study, the longitudinal changes of RV volumes and function in a large cohort of patients with HLHS after TCPC completion are demonstrated. The study results expand the available literature with the following main findings: 1) during long-term follow-up, there is an increase of indexed RV volumes in HLHS patients along with a mild but not significant decrease in RVEF and LAS, 2) indexed RV volumes mildly correlate with RVEF and LAS 3) CMR-derived LAS might be useful to assess RV function and is a promising marker for longitudinal contractile function in future studies as it correlates with RVEF and is easy to measure.

### 4.1 Importance of ventricular function in single ventricle patients

Despite advances in surgical management and post-operative follow-up, HLHS remains a complex disease that carries substantial morbidity and mortality. Well-described risk factors for worse survival in Fontan patients include prematurity, genetic syndromes, restrictive atrial septum and right ventricular (RV) dysfunction (Son JS et al., 2018). Accurate evaluation of RV volumes and function in these patients forms an essential aspect of surgical planning, peri-operative care and long-term management and is increasingly recognized as having prognostic significance in various disease processes (Zaidi SJ et al., 2018) (Fonseca BM, 2013) (Bell A et al., 2014).

### 4.2 Methods to evaluate ventricular function in single ventricle patients

In HLHS, long-term outcome is closely related to RV function. In clinical practice RV function is mostly analyzed qualitatively by transthoracic echocardiography. Simple indices such as LAS, TAPSE and RVEF are used, however, they are often subjective in HLHS

patients. In addition, acquiring these indices by transthoracic echocardiography have the limitations of angle dependency and a significant degree of inter-user variability (**Bellsham-Revell HR et al., 2013**).

CMR demonstrated to be accurate and reproducible for the assessment of RV volumes, EF and mass as well as TAPSE and LAS in patients with a biventricular circulation (**Shang Y et al., 2022**). Studies in HLHS showed the potential utility of TAPSE as a descriptor of ventricular performance in the population of children and adolescents with HLHS after Fontan operation (**Avitabile et al., 2014**) (**Goldberg DJ et al., 2016**) (**Morcos et al., 2009**). TAPSE quantifies the longitudinal shortening of the RV, accepted as a simple, reproducible, reliable method for estimating RV function and correlates well with exercise capacity and important markers of function outcome in healthy adults (**Zhao H et al., 2019**) (**Goldberg DJ et al., 2016**).

In the present study we demonstrated that TAPSE correlates with RV function in patients with HLHS after Fontan operation, but that there is no association between TAPSE and RVEF. This is similar to studies from Avitabile et al. Goldberg et al. and Morcos et al. (**Avitabile et al., 2014**) (**Goldberg DJ et al., 2016**) (**Morcos et al., 2009**). Largely preserved RVEF despite diminished longitudinal shortening as found in our group may suggest that global function of the systemic RV may be more dependent on radial or circumferential contraction. (**Goldberg DJ et al., 2016**) (**Avitabile et al., 2014**) (**Morcos PG et al., 2009**) (**Zhao H et al., 2019**).

We also demonstrated that LAS is a promising marker for longitudinal contractile function and is suited for the assessment in HLHS patients and correlates with RVEF. This is compatible with studies of Arenja et al. and Riffel et al. as well as Shang Y study showed LAS has been proposed as an accurate and simple measure of RV function, and correlated well with RVEF (**Arenja et al., 2016**) (**Riffel et al., 2015**) (**Shang Y et al., 2022**).

Abraham et al and Kanngiesser et al. showed that Speckle tracking echocardiography and CMR-based feature-tracking are tools that might be able to detect early alterations in RV myocardial deformation and function (**Abraham et al., 2007**) (**Kanngiesser et al., 2022**).

Gasparini et al. performed a systematic review to evaluate how strain measurements with cardiac magnetic resonance feature tracking could be used to evaluate right ventricular function in patients with HLHS patients (**Gasparini M et al., 2021**). They were able to show that cardiac magnetic resonance feature tracking for RV strain analysis can be used in patients with HLHS for early detection of ventricular dysfunction alongside clinical symptoms and EF values (**Gasparini M et al., 2021**).

In patients with HLHS, RV function and segmental deformation may be affected by LV morphology before and after Fontan palliation. In this context Wang et al. could show that patients with an absent or slitlike LV had better average RV systolic function (**Wang AP et al., 2021**). However, the long-term effect of LV morphology is still unknown.

### **4.3 Serial changes in RV volumes and mass**

There is a gap of knowledge regarding the fate of the single right ventricle in HLHS patients during long-term follow-up. It is, however, of importance to improve our understanding of the longitudinal performance of the single RV in this patient group for the early detection of adverse RV remodeling and to improve patient management. In this study, we reported longitudinal data about RV dimensions and mass in HLHS patients after Fontan completion and were able to demonstrate that there is a significant increase in BSA normalized RV volumes over time in older patients with an age of above 10 years.

Serial RV changes in HLHS patients have been reported by other authors; however, the majority of studies focused on RV changes throughout the staged palliation (**Bellsham-Revell et al., 2013; Kutty et al., 2012; Khoo et al, 2011; Son et al., 2018**), whereas we included paediatric and adult patients after completed three stage palliation.

Latus et al collected CMR data on single ventricular function in a mixed cohort of single LV and single RV Fontan patients and found, similarly to our study, an increase in RVEDVi in patients with a single RV during follow-up (**Latus et al., 2020**). That ventricular size is associated with ventricular outcome in Fontan patients has been shown by Rathod et al. who retrospectively assessed CMR data from a group of 215 Fontan patients and found that EDVi is an independent predictor of transplant-free survival after Fontan completion (**Rathod et al., 2014**). Therefore, they pointed out that measuring ventricular size by CMR is of clinical importance. The main finding of our study was a significant increase in RV indexed volumes over time in patients with an age >10 years. Van den Eynde et al. discussed in his letter that RV dilation might begin after 10 years of age due physiological changes associated with puberty such as the increase in blood pressure with associated increased afterload (**Van den Eynde J, et al 2022**). They refer to a study by Lui et al. that showed that puberty might impact RV fate in older children with cyanotic CHD by suppressing myocardial hypoxia-inducible factor (HIF-1 $\alpha$ ), which regulates the adaptive metabolic program to maintain relatively normal ATP production and cardiac function in chronic hypoxia hearts by increasing glycolysis and glucose oxidation and by inhibiting fatty acid oxidation. HIF-1 $\alpha$  signaling might be suppressed by insulin resistance during puberty, which is associated with cardiac metabolic maladaptation and cardiac dysfunction (**Liu Y et al., 2021**).

However, in our study the patient group with an age <10 years was relatively small. Therefore, it should be considered that significant changes in young patients could have been detected with a larger sample and, thus, increased power. We found only a mild increase in RVMMi during follow-up, but this finding was not significant. Similarly, there was no significant change in RSVVi throughout the examinations.

#### **4.4. Serial changes RV ejection fraction and LAS**

Serial assessment of RV function is essential in children with HLHS following surgical palliation with the TCPC, due to the complex geometry of the single RV (Mahle et al., 2001) and the expected development of RV dysfunction. Attrition of ventricular function is well recognized among Fontan patients, but early detection of ventricular dysfunction is difficult (Meyer et al., 2020). A recent multicenter study in a large and mixed cohort of Fontan patients demonstrated a decrease of ventricular ejection fraction over time (Atz et al., 2017). However, ventricular functional data in HLHS patients after TCPC completion are sparse. An echocardiographic study from our institution reported longitudinal data on a smaller cohort of patients with HLHS. It could be demonstrated that global strain rate parameters decreased significantly from 1.6 years to 5.1 years after TCPC, whereas there was no change in traditional echocardiographic parameters such as fractional area change (Michel et al., 2016). Meyer et al. in prospective follow-up study in Fontan patients, age  $\geq 10$  years reported a decrease in cardiac strain over 2 years in Fontan patients without clinical signs of Fontan failure, where EF, CI and clinical status were still preserved and concluded that cardiac strain might be a sensitive early indicator of systolic ventricular decline (Meyer et al., 2020).

In this study, we investigated a larger cohort of patients during a longer follow-up period and could demonstrate only a mild decrease in RVEF and LAS over time. A potential reason might be that the type of adaption of the systemic RV myofibers to systemic pressures allows to maintain a reasonable cardiac function during medium-term follow-up ( Bellsham-Revell HR et al., 2013) ( Khoo NS et al., 2011).

Future research needs to investigate a longer follow-up period and it might be of interest to assess additional parameters of RV regional function. We demonstrated that moderate tricuspid regurgitation was associated with higher RVEDVi and RVESVi compared to less degrees of tricuspid regurgitation, but this difference was not significant while the degree of tricuspid regurgitation did not have any impact on RVEF and LAS. In Fontan patients, the EF

was found to be stable over 15 years of follow-up (**Nakamura et al., 2011**). Therefore, size may be a better marker than EF.

CMR is the gold standard for the measurement of ventricular volumes and EF, and it also allows to easily measure LAS (**Riffel et al., 2015; Arenja et al., 2017**). We could demonstrate that LAS is suited for the assessment in HLHS patients and correlates with RVEF. Therefore, it seems suitable to add these parameters to future serial studies in HLHS patients. However, giving the fact that we could only observe significant changes for indexed RV volumes over time along with good correlations with RVEF as well as LAS (Figure 9 A), we suggest, that RVEDVi and RVESVi are superior markers to monitor the right ventricle in HLHS patients.

#### **4.5 Limitations**

This is a retrospective study with all its inherent limitations. Compared to the number of patients who had two examinations, the number of patients who had three CMR examinations is smaller, and this might have had an impact on the study results. However, to our knowledge, this is the largest study investigating longitudinal geometry and function in HLHS patients using CMR.

The impact of additional interventions and surgeries between the CMR examinations as well as the effect of an open fenestration was not assessed in this study. Aortopulmonary collaterals are common in Fontan patients and may account for volume loading over time. In particular older CMR examinations included in our analysis did not include enough data to calculate pulmonary collateral flow and therefore we are unable to provide follow-up data on this measure. In addition, we did not investigate the effect of an ACEi therapy on volumetric measurements and data from cardiac catheterisation, cardiopulmonary exercise testing as well as adverse events were also not considered in our analysis. Although we started routine measurements of N-terminal pro B-type natriuretic peptide (NT-proBNP) ~5 years ago, the

number of patients with available results was relatively small and therefore we decided to exclude these data.

LAS was measured for a more comprehensive assessment of RV function. However, it has to be acknowledged that it is an extrapolation of an LV functional parameter. Both, LAS and RVEF are load dependent markers that can be influenced by tricuspid valve regurgitation, we did not analyse load-independent parameters. Sedation was necessary in 162 children. Although we believe that the effect of sedation is negligible, we cannot exclude an impact on ventricular volumes.

## 5. SUMMARY

HLHS is one of the most severe forms of congenital heart disease and is characterized by hypoplasia of the left ventricle, mitral valve and aortic valve atresia or stenosis as well as hypoplasia of the ascending aorta.

Neonates with HLHS are critically ill and will need to be managed in the intensive care unit and stabilized before surgical intervention include maintaining ductal patency, avoid excess pulmonary blood flow, and ensure adequate blood flow from the left atrium to the right atrium.

The Norwood operation in many cardiac centers, is the surgical palliation of choice followed by an upper cavopulmonary connection and completion of the Fontan circulation by creation of a total cavopulmonary connection (TCPC).

The outcome after Fontan operations shows a clear trend toward improved early and long-term survival. However, specialized long-term follow-up is paramount for detection of early RV failure and other Fontan associated complications.

Accurate evaluation of RV function based on simplified geometrical models is difficult due to RV shape and its coarse trabeculations and is even more challenging for the single RV in patients with HLHS. CMR is the gold standard for the assessment of RV volumes and function, and this includes patients with HLHS as CMR provides accurate visualisation of the entire RV chamber. So far, only few studies have evaluated RV function in HLHS patients after TCPC completion and most of them included other single ventricle patients.

The present work aimed to fill this gap by assessing RV volumes and RV functional markers from serial cardiovascular magnetic resonance (CMR) studies in a large cohort of HLHS patients after completion of the TCPC.

Inclusion criteria were HLHS patients who had at least 2 serial CMR studies after Fontan completion with a four-chamber cine view to measure long-axis strain (LAS) and/or a

complete stack of short-axis cines for RV volumetry. Exclusion criteria were patients with only one CMR study and insufficient data sets for the analysis of RV volumes and/or LAS.

Sixty patients had two examinations and thirty-five patients had three CMR examinations. All patients underwent Fontan completion with TCPC at a median age of 2.7. Median age and interquartile range (IQR) of included patients at the three examinations was 4.2 [3.3; 6.1] years, 9.4 [5.7; 11.4] years and 14.6 [11.8; 16.8] years. The oldest patient at the time of the third examination was 21.2 years.

RV volumes were measured from manual tracing of endocardial contours for each slice from the stack of short-axis cine images at end-systole and end-diastole using Simpson's method. TAPSE and LAS were measured from a standard apical four-chamber view.

There was a significant increase in RV indexed end-systolic and end-diastolic volumes (RVEDVi, RVESVi) from the first to the second as well as from the first and the second examination to the third examination in patients with an age >10 years.

Good-to excellent interobserver agreement was shown for all right ventricular measurements in 25 patients. The intra-class correlation coefficient ranged from 0.78 to 0.996. There was no significant change for indexed RV stroke volume throughout the examinations.

The main finding of our study was a significant increase in RV indexed volumes over time in patients with an age >10 years only a mild decrease in RVEF and LAS over time.

LAS correlated with correlated with RVEF suggesting that it might be a suitable marker for RV assessment in HLHS patients. Therefore, our results suggest that indexed RV volumes might be best to monitor the RV in patients with HLHS.

Future research needs to investigate a longer follow-up period and it might be of interest to assess additional parameters of RV regional function and to investigate the influence of anatomical HLHS subtypes.

## 6. List of Literature

Baumgartner H, De Backer J, Babu-Narayan SV, Budts W, Chessa M, Gerhard-Paul Diller GP et al. 2020 ESC Guidelines for the Management of Adult Congenital Heart Disease: The Task Force for the Management of Adult Congenital Heart Disease of the European Society of Cardiology (ESC)(2020). *Eur Heart J* 29: [Epub ahead of print].

Abouzeid CM, Shah T, Johri A, Weinsaft JW, Kim J. Multimodality Imaging of the Right Ventricle. *Curr Treat Options Cardiovasc Med*. 2017;19:82.

Abraham TP, Dimaano VL, Liang HY. Role of tissue Doppler and strain echocardiography in current clinical practice. *Circulation*. 2007;116:2597-2609.

Akkinapally S, Hundalani SG, Kulkarni M, Fernandes CJ, Cabrera AG, Shivanna B et al. Prostaglandin E1 for maintaining ductal patency in neonates with ductal-dependent cardiac lesions. *Cochrane Database Syst Rev*. 2018 Feb; 2018(2): CD011417.

Alabdulgader AA. Survival analysis: Prenatal vs. postnatal diagnosis of HLHS. *J Invasive Noninvasive Cardiol*. 2018;1:8-12.

Anderson PA, Sleeper LA, Mahony L, Colan SD, Atz AM, Breitbart RE et al. Contemporary outcomes after the Fontan procedure: a Pediatric Heart Network multicenter study. *J Am Coll Cardiol*. 2008;52: 85–98.

Anderson RH, Herberg U, Simpson J, Bellsham-Revell H, Galletti L, Schranz D et al. Guidelines to hypoplastic left heart syndrome. *Eur J Cardiothorac Surg*. 2021;59:924-925.

Arenja N, Riffel JH, Djiokou CN, Florian Andre F, Fritz T, Halder M et al. Right ventricular long axis strain—validation of a novel parameter in non-ischemic dilated cardiomyopathy using standard cardiac magnetic resonance imaging. *Eur J Radiol.* 2016;85:1322-1328.

Arenja N, Riffel JH, Fritz T, André F, Aus dem Siepen F, Mueller-Hennessen M et al. Diagnostic and Prognostic Value of Long-Axis Strain and Myocardial Contraction Fraction Using Standard Cardiovascular MR Imaging in Patients with Nonischemic Dilated Cardiomyopathies. *Radiology.* 2017;283:681-691.

Atz AM, Zak V, Mahony L, Uzark K, D'agincourt N, Goldberg DJ, Williams RV et al. Longitudinal outcomes of patients with single ventricle after the Fontan procedure. *J Am Coll Cardiol.* 2017;69:2735-2744.

Avitabile CM, Whitehead K, Fogel M, Mercer-Rosa L. Tricuspid Annular Plane Systolic Excursion Does Not Correlate with Right Ventricular Ejection Fraction in Patients With Hypoplastic Left Heart Syndrome After Fontan Palliation. *Pediatr Cardiol.* 2014;35:1253-1258.

Bautista-Hernandez V, Avila-Alvarez A, Marx GR, Nido PJD. Current surgical options and outcomes for newborns with hypoplastic left heart syndrome. *An Pediatr (Engl Ed).* 2019;91:352.e1-352.e9.

Bell A, Rawlins D, Bellsham-Revell H, Miller O, Razavi R, Simpson J. Assessment of right ventricular volumes in hypoplastic left heart syndrome by real-time three-dimensional echocardiography: comparison with cardiac magnetic resonance imaging. *Eur Heart J Cardiovasc Imaging.* 2014;15:257-266.

Bellsham-Revell H. Noninvasive Imaging in Interventional Cardiology: Hypoplastic Left Heart Syndrome. *Front Cardiovasc Med.* 2021; 8:637838.

Bellsham-Revell HR, Tibby SM, Bell AJ, Witter T, Simpson J, Beerbaum P et al. Serial Magnetic Resonance Imaging in Hypoplastic Left Heart Syndrome Gives Valuable Insight into Ventricular and Vascular Adaptation. *J Am Coll Cardiol.* 2013;61:561-570.

Best KE, Miller N, Draper E, Tucker D, Luyt K, Rankin J. The Improved Prognosis of Hypoplastic Left Heart: A Population-Based Register Study of 343 Cases in England and Wales. *Front Pediatr.* 2021;9:635776.

Budts W, Roos-Hesselink J, Radle-Hurst T, Eicken A, McDonagh TA, Lambrinou E, et al. Treatment of heart failure in adult congenital heart disease: a position paper of the Working Group of Grown-Up Congenital Heart Disease and the Heart Failure Association of the European Society of Cardiology. *Eur Heart J.* 2016;37:1419-1427.

D'Alto M, Dimopoulos K, Budts W, Diller GP, Di Salvo G, Dellegrottaglie S, et al. Multimodality imaging in congenital heart disease-related pulmonary arterial hypertension. *Heart.* 2016;102(9):910-8.

Dessardo S, Ahel V. Preoperative management of hypoplastic left heart syndrome. *SIGNA VITAE* 2009;4: 12-15.

Devos DG, Kilner PJ. Calculations of cardiovascular shunts and regurgitation using magnetic resonance ventricular volume and aortic and pulmonary flow measurements. *Eur Radiol.* 2010;20:410-421.

Driscoll DJ, Offord KP, Feldt RH, Schaff HV, F J Puga FJ, Danielson GK, et al. Five- to fifteen-year follow-up after Fontan operation. *Circulation.* 1992;85:469-496.

Eckhauser A, Pasquali SK, Ravishankar C, Lambert LM, Newburger JW, Atz AM, et al. Variation in care for infants undergoing the stage II palliation for hypoplastic left heart syndrome. *Cardiol Young*. 2018;28:1109-1115.

Edelson JB, Ravishankar C, Griffis H, Zhang X, Faerber J, Gardner MM, et al. A Comparison of Bidirectional Glenn vs. Hemi-Fontan Procedure: An Analysis of the Single Ventricle Reconstruction Trial Public Use Dataset. *Pediatr Cardiol*. 2020;41:1166-1172.

Erikssen G, Aboulhosn J, Lin J, Liestøl K, Estensen ME, Gjesdal O, et al. Survival in patients with univentricular hearts: the impact of right versus left ventricular morphology. *Open Heart*. 2018;5: e000902.

Feinstein JA, Benson DW, Dubin AM, Cohen MS, Maxey DM, Mahle WT, et al. Hypoplastic Left Heart Syndrome: Current Considerations and Expectations. *J Am Coll Cardiol*. 2012;59(1 Suppl): S1-42.

Fonseca BM. Perioperative imaging in hypoplastic left heart syndrome. *Semin Cardiothorac Vasc Anesth*. 2013;17:117-127.

Garcia AM, Beatty JT, Nakano SJ. Heart failure in single right ventricle congenital heart disease: physiological and molecular considerations. *Am J Physiol Heart Circ Physiol*. 2020;318:H947-H965.

Gasparini M, Cox N. Role of cardiac magnetic resonance strain analysis in patients with hypoplastic left heart syndrome in evaluating right ventricular dysfunction: a systematic review. *Eur J Cardiothorac Surg*. 2021;60:497-505.

Goldberg DJ, French B, Szwast AL, McBride MG, Stephen M, Paridon SM, et al. Tricuspid Annular Plane Systolic Excursion Correlates with Exercise Capacity in a Cohort of Patients with

Hypoplastic Left Heart Syndrome After Fontan Operation. *Echocardiography*; 2016;33:1897–1902.

Graupner O, Enzensberger C, Fliedner RA. New Aspects in the Diagnosis and Therapy of Fetal Hypoplastic Left Heart Syndrome. *Geburtshilfe Frauenheilkd*. 2019;79:863–72.

Hansen JH, Petko C, Bauer G, Voges I, Kramer HH, Scheewe J. Fifteen-year single-center experience with the Norwood operation for complex lesions with single-ventricle physiology compared with hypoplastic left heart syndrome. *J Thorac Cardiovasc Surg*. 2012; 144:166–172.

Husain N, Gokhale J, Nicholson L, Cheatham JP, Holzer RJ, Cua CL. Noninvasive estimation of ventricular filling pressures in patients with single right ventricles. *J Am Soc Echocardiogr* 2013;26:1330-1336.

Iriart X, Roubertie F, Jalal Z, Thambo J. Quantification of systemic right ventricle by echocardiography. *Arch Cardiovasc Dis*. 2016;109:120-127.

Jacobs JP, Mayer JE, Pasquali SK, Hill KD, Overman DM, St Louis JD, et al. The Society of Thoracic Surgeons Congenital Heart Surgery Database: 2019 Update on Outcomes and Quality. *Ann Thorac Surg*. 2019;107:691-704.

Johnson J, Connolly HM. Overview of the management and prognosis of patients with Fontan circulation. UpToDate. Retrieved Feb 2022, Available from <https://www.uptodate.com/contents/overview-of-the-management-and-prognosis-of-patients-with-fontan-circulation>.

Johnson J, Veldtman G. Management of complications in patients with Fontan circulation.

UpToDate. Retrieved May 2022, Available from

<https://www.uptodate.com/contents/overview-of-the-management-and-prognosis-of-patients-with-fontan-circulation>.

Kanngiesser LM, Freitag-Wolf S, Boroni Grazioli S, Gabbert DD, Uebing AS, Voges I. Serial Assessment of Right Ventricular Deformation in Patients With Hypoplastic Left Heart Syndrome: A Cardiovascular Magnetic Resonance Feature Tracking Study. *J Am Heart Assoc*. 2022;11:e025332.

Khoo NS, Smallhorn JF, Kaneko S, Myers K, Kutty S, Tham EB. Novel insights into RV adaptation and function in hypoplastic left heart syndrome between the first 2 stages of surgical palliation. *JACC Cardiovasc Imaging*. 2011;4:128-37.

Kończ J, Skalski J. Contemporary strategies of the hypoplastic left heart syndrome treatment. *Kardiol Pol*. 2011;69:275–280.

Kritzmire SM, Cossu AE. Hypoplastic Left Heart Syndrome. In: StatPearls [Internet]. Treasure Island (FL): StatPearls Publishing; 2022 Jan–. PMID: 32119463.

Kutty S, Graney BA, Khoo NS, Li L, Polak A, Gribben P, et al. Serial Assessment of Right Ventricular Volume and Function in Surgically Palliated Hypoplastic Left Heart Syndrome Using Real-Time Transthoracic Three-Dimensional Echocardiography. *J Am Soc Echocardiogr*. 2012 ;25:682-689.

Kverneland LS, Kramer P, Ovrouski S. Five decades of the Fontan operation: A systematic review of international reports on outcomes after univentricular palliation. *Congenit Heart Dis*. 2018;13:181-193.

Latus H, Kruppa P, Hofmann L, Reich B, Jux C, Apitz C, et al. Impact of aortopulmonary collateral flow and single ventricle morphology on longitudinal hemodynamics in Fontan patients: A serial CMR study. *Int J Cardiol.* 2020;311:28-34.

Leiner T, Bogaert J, Friedrich MG, Mohiaddin R, Muthurangu V, Myerson S, et al. SCMR Position Paper on clinical indications for cardiovascular magnetic resonance. *J Cardiovasc Magn Reson.* 2020;22:76.

Leirgul E, Fomina T, Brodwall K, Greve G, Holmstrom H, Vollset SE, et al. Birth prevalence of congenital heart defects in Norway 1994-2009—a nationwide study. *Am Heart J.* 2014;168:956-964.

Licht DJ, Shera DM, Clancy RR, Wernovsky G, Montenegro LM, Nicolson SC, et al. Brain maturation is delayed in infants with complex congenital heart defects. *J Thorac Cardiovasc Surg.* 2009;137(3):529-536.

Liu Y, Luo Q, Su Z, Xing J, Wu J, Xiang L, et al. Suppression of Myocardial Hypoxia-Inducible Factor-1 $\alpha$  Compromises Metabolic Adaptation and Impairs Cardiac Function in Patients with Cyanotic Congenital Heart Disease During Puberty. *Circulation.* 2021;143:2254-2272.

Mahle WT, Coon PD, Wernovsky G, Rychik J. Quantitative echocardiographic assessment of the performance of the functionally single right ventricle after the Fontan operation. *Cardiol Young.* 2001;11:399-406.

Marelli AJ, Mackie AS, Ionescu-Ittu R, Rahme E, Pilote L. Congenital heart disease in the general population: changing prevalence and age distribution. *Circulation.* 2007;115:163-172.

McCrindle BW, Williams RV, Mital S, Clark BJ, Russell JL, Klein G, et al. Physical activity levels in children and adolescents are reduced after the Fontan procedure, independent of exercise capacity, and are associated with lower perceived general health. *Arch Dis Child*. 2007;92:509-514.

Meyer SL, Ridderbos FS, Wolff D, Eshuis G, Melle JPV, Ebels T, et al. Serial cardiovascular magnetic resonance feature tracking indicates early worsening of cardiac function in Fontan patients. *Int J Cardiol*. 2020;303:23-29.

Michel M, Logoteta J, Entenmann A, Hansen JH, Voges I, Kramer HH, et al. Decline of Systolic and Diastolic 2D Strain Rate During Follow-Up of HLHS Patients After Fontan Palliation. *Pediatr Cardiol*. 2016;37:1250-1257.

Miller JR, Simpson KE, Epstein DJ, Lancaster TS, Henn MC, Schuessler RB, et al. Improved survival after heart transplant for failed Fontan patients with preserved ventricular function. *J Heart Lung Transplant*. 2016;35:877-883.

Morcos PG, Vick GW, Sahn DJ, Jerosch-Herold M, Shurman A, Sheehan FH. Correlation of right ventricular ejection fraction and tricuspid annular plane systolic excursion in tetralogy of Fallot by magnetic resonance imaging. *Int J Cardiovasc Imaging*. 2009 Mar;25(3):263-70.

Nakamura Y, Yagihara T, Kagisaki K, Hagino I, Kobayashi J. Ventricular performance in long-term survivors after Fontan operation. *Ann Thorac Surg*. 2011;91:172-80.

Ono M, Boethig D, Goerler H, Lange M, Westhoff-Bleck M, Breymann T. Clinical outcome of patients 20 years after Fontan operation--effect of fenestration on late morbidity. *Eur J Cardiothorac Surg*. 2006;30:923-929.

Rai V, Gładki M, Dudyńska M, Skalski J. Hypoplastic left heart syndrome [HLHS]: treatment options in present era. *Indian J Thorac Cardiovasc Surg.* 2019;35:196-202.

Rao PS. Management of Congenital Heart Disease: State of the Art-Part II-Cyanotic Heart Defects. *Children (Basel).* 2019;6:54.

Rathod RH, Fulton DR, Armsby C. Hypoplastic left heart syndrome: Anatomy, clinical features, and diagnosis. UpToDate. Retrieved May 2022. Available from <https://www.uptodate.com/contents/hypoplastic-left-heart-syndrome-anatomy-clinical-features-and-diagnosis>.

Rathod RH, Prakash A, Kim YY, Germanakis IE, Powell AJ, Gauvreau K, et al. Cardiac magnetic resonance parameters predict transplantation-free survival in patients with fontan circulation. *Circ Cardiovasc Imaging.* 2014;7:502-509.

Rathod RH, Prakash A, Powell AJ, Geva T. Myocardial Fibrosis Identified by Cardiac Magnetic Resonance Late Gadolinium Enhancement is Associated with Adverse Ventricular Mechanics and Ventricular Tachycardia Late After Fontan Operation *J Am Coll Cardiol.* 2010;55:1721-1728.

Reller M, Strickland MJ, Riehle-Colarusso T, Mahle WT, Correa A. Prevalence of congenital heart defects in metropolitan Atlanta, 1998-2005. *J Pediatr.* 2008;153:807-813

Riffel JH, Andre F, Maertens M, Rost F, Keller MG, Giusca S, et al. Fast assessment of long axis strain with standard cardiovascular magnetic resonance: a validation study of a novel parameter with reference values. *J Cardiovasc Magn Reson.* 2015;17:69.

Roeleveld PP, Axelrod DM, Klugman D, Jones MB, Chanani NK, Rossano JW, et al. Hypoplastic left heart syndrome: from fetus to fontan. *Cardiol Young.* 2018;28:1275-1288.

Rychik J, Atz AM, Celermajer DS, Deal BJ, Gatzoulis MA, Gewillig MH, et al. Evaluation and Management of the Child and Adult With Fontan Circulation: A Scientific Statement From the American Heart Association. *Circulation*. 2019; CIR00000000000000696.

Salehi Ravesh M, Rickers C, Bannert FJ, Hautemann D, Al Bulushi A, Gabbert DD, et al. Longitudinal Deformation of the Right Ventricle in Hypoplastic Left Heart Syndrome: A Comparative Study of 2D-Feature Tracking Magnetic Resonance Imaging and 2D-Speckle Tracking Echocardiography. *Pediatr Cardiol*. 2018;39:1265-1275.

Samarai D, Ingemansson SL, Gustafsson R, Thilén U, Hlebowicz J. Global longitudinal strain correlates to systemic right ventricular function. *Cardiovasc Ultrasound*. 2020;18:4.

Santens B, Van De Bruaene A, Koestenberger M, Hansmann G, Budts W, Bernstein D, et al. Diagnosis and treatment of right ventricular dysfunction in congenital heart disease. *Cardiovasc Diagn Ther*. 2020;10:1625-1645.

Schlangen J, Petko C, Hansen JH, Michel M, Hart C, Uebing A, et al. Two-dimensional global longitudinal strain rate is a preload independent index of systemic right ventricular contractility in hypoplastic left heart syndrome patients after Fontan operation. *Circ Cardiovasc Imaging*. 2014;7:880-886.

Schneider M, Beichl M, Nietsche C, Beitzke D, Porenta G, Beran G, et al. Systematic Evaluation of Systemic Right Ventricular Function. *J Clin Med*. 2019;9:107.

Schneider M, Ran H, Aschauer S, Binder C, Mascherbauer J, Lang I, et al. Visual assessment of right ventricular function by echocardiography: How good are we? *Int J Cardiovasc Imaging*. 2019;35:2001-2008.

Schranz D, Bauer A, Reich B, Steinbrenner B, Recla S, Schmidt D, et al. Fifteen-year Single Center Experience with the “Giessen Hybrid” Approach for Hypoplastic Left Heart and Variants: Current Strategies and Outcomes. *Pediatr Cardiol.* 2015;36:365-373.

Shang Y, Zhang Y, Leng W, Lei X, Chen L, Zhou X, et al. Assessment of right ventricular function using cardiovascular magnetic resonance in patients with type 2 diabetes mellitus. *Quant Imaging Med Surg.* 2022;12:1539-1548.

Siffel C, Riehle-Colarusso T, Oster ME, Correa A. Survival of Children With Hypoplastic Left Heart Syndrome. *Pediatrics.* 2015;136:e864-70

Sobh M, Freitag-Wolf S, Scheewe J, Kanngiesser LM, Uebing AS, Voges I. Serial right ventricular assessment in patients with hypoplastic left heart syndrome: a multiparametric cardiovascular magnetic resonance study. *Eur J Cardiothorac Surg.* 2021;61:36-42.

Son JS, James A, Fan CS, Mertens L, McCrindle BW, Manlhiot C, et al. Prognostic Value of Serial Echocardiography in Hypoplastic Left Heart Syndrome. *Circ Cardiovasc Imaging.* 2018;11:e006983.

Stout KK, Daniels CJ, Aboulhosn JA, Bozkurt B, Broberg CS, Colman JM, et al. AHA/ACC Guideline for the Management of Adults With Congenital Heart Disease: A Report of the American College of Cardiology/American Heart Association Task Force on Clinical Practice Guidelines. *J Am Coll Cardiol.* 2019;73:e81-e192.

Tweddell JS, Hoffman GM, Ghanayem NS, Frommelt MA, Kathleen A, Mussatto KA, et al. Hypoplastic left heart syndrome. In: Moss and Adams' Heart Disease in Infants, Children and Adolescents: Including the Fetus and Young Adult, 10th ed, Shaddy RE, Penny DJ, Feltes TF,

et al. (Eds), Lippincott Williams & Wilkins, Philadelphia 2021. Copyright © 2021 Lippincott Williams & Wilkins. [www.lww.com](http://www.lww.com).

VanderWeele TJ, Mathur MB. Some desirable properties of the bonferroni correction: is the bonferroni correction really so bad? *Am J Epidemiol*. 2019 Mar; 188(3): 617–618.

Van den Eynde J, Danford DA, Doshi A, Kutty S. Right ventricular dysfunction in hypoplastic left heart syndrome: superimposed effects of afterload and insulin resistance in puberty?. *Eur J Cardiothorac Surg*. 2022;ezac088

Wang AP, Kelle AM, Hyun M, Reece CL, Young PM, O'Leary PW, et al. Wanek Family Program for Hypoplastic Left Heart Syndrome Imaging Pipeline. Negative Impact of the Left Ventricular Remnant Morphology on Systemic Right Ventricular Myocardial Deformation in Hypoplastic Left Heart Syndrome. *Pediatr Cardiol*. 2021;42:278-288.

Wilson TG, Iyengar AJ, Winlaw DS, Weintraub RG, Wheaton GR, Gentles TL, et al. Use of ACE inhibitors in Fontan: Rational or irrational? *Int J Cardiol*. 2016;210:95-99.

Zaidi SJ, Penk J, Cui VW, Kanjanauthai S, Roberson DA. Right Ventricular Systolic Function Parameters in Hypoplastic Left Heart Syndrome. *Pediatr Cardiol*. 2018;39:1423-1432.

Zhao H, Kang Y, Pickle J, Wang J, Han Y. Tricuspid annular plane systolic excursion is dependent on right ventricular volume in addition to function. *Echocardiography*. 2019;36:1459-1466.